UNIVERSITY OF KWAZULU-NATAL ™

INYUVESI YAKWAZULU-NATALI

Ursolic acid as a potential inhibitor of *Mycobacterium tuberculosis* cytochrome *bc1* oxidase: A molecular modelling perspective

by

Ntombikayise Tembe

219094557

A dissertation submitted in partial fulfilment of the requirements for the degree of

Master of Medical Science.

College of Health Sciences

School of Laboratory Medicine & Medical Sciences

Department of Medical Biochemistry

University of KwaZulu-Natal, Durban 4000, South Africa.

2021

Ursolic acid as a potential inhibitor of *Mycobacterium tuberculosis* cytochrome *bc1* oxidase: A molecular modelling perspective

by

Ntombikayise Tembe

219094557

A dissertation submitted in fulfilment of the academic requirements for the degree of

Master of Medical Science

2021

This is the thesis in which the chapters are written as a set of discrete research publications, with an overall introduction and final summary. Typically, these chapters will have been published in internationally recognized, peer-reviewed journals.

 This is to certify that the contents of this thesis are the original research work of **Miss Ntombikayise Tembe.**

Supervisor:

As the candidate's supervisor, I have approved this thesis for submission.

Dr Ndumiso N. Mhlongo   Signature: _____   Date: 04 November 2021

Co-Supervisor:

Dr Hezekiel M. Kumalo   Signature: _____   Date: 04 November 2021

PREFACE

This thesis is divided into four chapters:

Chapter 1: In this chapter, the background, aims and objectives, relevance as well as general outline and structure of the thesis is addressed.

Chapter 2: The background of the study is provided in this chapter. Updated statistics on TB number of infections and deaths worldwide are covered, as well as pathogenesis. The structure of *M. tuberculosis* QcrB is shown and enzymes involved in the progression of TB are highlighted. These enzymes serve as drug targets. Some medicinal plants that are known to cure TB are highlighted. Drugs targeting QcrB and natural compound structures are also shown. This chapter also provides an overview of computational chemistry, diverse molecular modelling and molecular simulation techniques, and their applications. Theoretical explanations have been provided for the computational methods. Following that, a discussion of the various computational tools used in TB research is provided, with a particular emphasis on molecular dynamics simulations, molecular docking, principal component analysis and molecular mechanics (QM/MM), and binding free energy calculations.

Chapter 3: Published manuscript **by the title; "Ursolic acid as a potential inhibitor of** *Mycobacterium tuberculosis* **cytochrome** *bc1* **oxidase, a molecular modelling perspective**".

Chapter 4: Conclusions and Future Prospects.

ABSTRACT

Tuberculosis (TB) is a disease, caused by an infectious agent; *Mycobacterium tuberculosis,* which persists as a major problem globally, especially in developing countries such as Brazil, Indonesia, and South Africa. Individuals who are diabetic and human immunodeficiency virus (HIV) co-infected are at a higher risk of contracting TB. Hence, these risk factors are associated with a compromised immune system. Among these factors, various strains are involved in the pathogenesis of TB such as multidrug-resistant tuberculosis (MDR-TB) and extensively drug-resistant tuberculosis (XDR-TB) strains. The emergence of these strains may result from failure to complete treatment within the stipulated period of six months. However, studies show that the protein QcrB; contributes more to TB pathogenesis. Therefore, there is an urgent need for the discovery of drugs that inhibit QcrB. The current FDA-approved anti-tubercular drugs such as, Lansoprazole sulfide (LSPZ) and Telacebec (Q203) which inhibit QcrB are bacteriostatic and have been linked to side effects including dementia, chronic kidney disease, and ischemic cardiac diseases [1], thus prompting a search for an alternative drug. Various natural compounds have been reported to possess several bioactivities that could be crucial in the management of tuberculosis (TB) disease. *Warbugia salutaris*, a medicinal plant has been found to exhibit inhibitory properties against *M. tuberculosis*. Numerous compounds are derived from *W. salutaris*. In this study, we focus solely on Ursolic acid (UA) and its derivative, Ursolic acid acetate (UAA). These two compounds possess antibacterial, anti-HIV, and antimycobacterial properties. This suggests that they could potentially possess inhibitory properties towards *M.tuberculosis* QcrB protein. In this study, computational methods are applied to investigate the inhibitory activity of UA and UAA *on M. tuberculosis* QcrB. Molecular Docking, Molecular Dynamics (MD) simulations, Radius of Gyration, Principal Component Analysis (PCA), and Molecular Mechanics-Generalized Born Surface Area (MM/GBSA) binding free energy calculations were performed in explicit solvent to

accomplish our goal. The obtained results indicated that the (1) the binding of UA to QcrB induced a more stable and compacted conformation compared to LSPZ and Q203; (2) high total binding free energy estimated in the QcrB-UA system was due to numerous hydrophobic residues in the binding site of QcrB that interact with phenyl rings of UA resulting in hydrophobic packing. This implies that UA has a high binding affinity and, as a result, a strong inhibition of QcrB; (3) more H-bonds were observed in the QcrB-UA system than in the QcrB-Q203 system; (4) rigidity was displayed mostly in Arg124 and Thr128; (5) Arg124 and Phe127 also contributed more to the total binding energy in QcrB-UA and QcrB-UAA. This implies that the ligands exert a high binding affinity in the porphyrin binding site than in the active site. The identification of a molecule that competes with the porphyrin ring for the binding site could be beneficial in QcrB pharmacological research; (6) UA could be a potential anti-tubercular agent through QcrB inhibition, although it is hepatotoxic within tolerable concentrations. However, observed potential hepatotoxicity was based on predictions. Although the preliminary findings of this report warrant further experimental validation, they lay a strong foundation for subsequent assessment and development of these natural compounds as anti-tubercular drugs.

DECLARATION 1- PLAGIARISM

I, **Ntombikayise Tembe**, declare that:

1. This dissertation contains original work conducted by the author and has not been submitted to UKZN or any other tertiary institution to obtain an academic qualification, whether by myself or any other party. The use of other people's work has been duly acknowledged in the text.

2. The research work presented in this study was carried out in the Department of Medical Biochemistry, School of Laboratory Medicine and Medical Science, Faculty of Health Sciences, University of KwaZulu-Natal, Durban, under the supervision of Dr N.N Mhlongo.

Signature with Date

Date: 26/10/2021

DECLARATION 2: PUBLICATION

Details of contribution to a publication that form part of the research presented in this thesis.

Publication 1

Ntombikayise Tembe, Kgothatso E. Machaba, Umar Ndagi, Hezekiel M. Kumalo and Ndumiso N. Mhlongo (2021). Ursolic acid as a potential inhibitor of *Mycobacterium tuberculosis* cytochrome *bc1* oxidase — a molecular modelling perspective, Journal of molecular modelling, Manuscript ID: JMMO-D-21-00139R1.

Authors' contributions:

Miss Ntombikayise Tembe: Conducted all calculations and manuscript writing.

Dr. Ndumiso N. Mhlongo.: Supervisor

Dr. Kgothatso E. Machaba.: Editing, manuscript revision and proofreading.

Dr Hezekiel M. Kumalo and Dr Umar Ndagi.: Manuscript proofreading.

ACKNOWLEDGEMENTS

DEDICATION

This dissertation is dedicated to:

My two lovely girls; Sinalo Senzelwa Madolo and Kungesihle Thandokuhle Madolo.

My late parents; Irene Tembe and Thembinkosi Tembe

LIST OF ABBREVIATIONS

Abbreviations	Full name
BA	Betulinic acid
EC	Eucosterol
FDA	Food and Drug Administration
IPG	Isopolygodial
LSPZ	Lansoprazole sulfide
MD	Molecular Dynamics
MDR-TB	Multidrug-resistant tuberculosis
MG	Muzigadial
MK	Mukaadial
MM/PBSA	Molecular Mechanics/ Poisson–Boltzmann Surface Area
MM/GBSA	Molecular Mechanics/ Generalised Born Surface Area
PCA	Principal Component Analysis
PG	Polygodial
PME	Particle Mesh Ewald
RMSF	Root Mean Square Fluctuation
RMSD	Root Mean Square Deviation

Rg   Radius of Gyration

ST   Salutarisolide

TB   Tuberculosis

UA   Ursolic acid

UAA   Ursolic acid acetate

UG   Ugandensidial

XDR-TB   Extensively drug-resistant tuberculosis

WB   Warbuganal

LIST OF FIGURES

LIST OF TABLES

Pages

TABLE OF CONTENTS

1. CHAPTER 1

INTRODUCTION

1.1   Background and rational of this study

Mycobacterium tuberculosis, a causative agent of tuberculosis disease, has been one of the leading causes of death worldwide since ancient times [1]. In 2019, an estimated 10.0 million individuals worldwide contracted TB, with 1.2 million deaths [2]. Diabetics who are also HIV co-infected are at a higher risk of contracting TB [3]. Diabetes increases susceptibility to tuberculosis via a variety of mechanisms such as hyperglycemia and cellular insulinopenia, both of which have indirect effects on macrophage and lymphocyte function [4]. HIV co-infected individuals often get infected with TB due to compromised immune systems. HIV promotes the progression of *M. tuberculosis* infection to active TB disease in both newly acquired and latent infections [5] [6]. TB, however, can be treated for 6 to 9 months with a combination of 4 drugs [5]. Multidrug-resistance (MDR) and extensively drug-resistance (XDR) TB have emerged as a result of improper use or inability to finish the full course of treatment [7]. As a result, effective treatments for both drug-sensitive and drug-resistant TB are in high demand. *M. tuberculosis* H37Rv is an obligate aerobe that generates energy via the electron transport chain and oxidative phosphorylation [8]. The beta subunit of cytochrome bc_1 oxidase plays a vital role in TB pathogenesis since it is involved in bacterial respiration [9]. FDA-approved drugs such as imidazo-pyrimidine amide (Q203) and lansoprazole sulfide (LSPZ) possess anti-tubercular activity against *M. tuberculosis* by targeting a beta subunit of the cytochrome bc_1 complex which is encoded by the gene QcrB, as well as causing a rapid ATP depletion [10] [8]. Q203 and LSPZ are bacteriostatic [11] and are linked to side effects such as dementia, chronic kidney disease, and ischemic cardiac diseases [12]. As a result, novel

1

TB drugs with fewer side effects, preferably derived from natural sources are required. Medicinal plants have been extensively used by ancient cultures to prevent and also cure a variety of common and deadly diseases including TB [13]. Natural compounds isolated from *Warbugia salutaris* have been reported to exhibit anti-mycobacterial activity [14]. These compounds include warburganal (WB) [15], polygodial (PG) [16], salutarisolide (ST) [17] [18], muzigadial (MG) [19], ugandensidial (UD), isopolygodial (IPG), mukaadial (MK) [20], betulinic acid (BA) and ursolic acid (UA) [21] [22]. Ursolic acid acetate (UAA) is a derivative of UA. *In silico* methods are a viable alternative approach for drug discovery and development. *In silico* methods save both time and cost, as drug discovery is both costly and time-consuming [23]. Molecular dynamic (MD) simulations are new *in silico* techniques with potential applications in a variety of areas of pharmacology [24] [25] [26]. The molecular docking method is used to model ligand-receptor interactions, allowing for the characterization of their association as well as the elucidation of fundamental biochemical processes involved [27]. The identification of ligand-receptor interactions is critical for rational drug design [28]. However, the results of molecular docking may be incorrect and thus require validation [29]. MM/GBSA and MM/PBSA (MM/PB(GB)SA) may be performed to validate their accuracy [30]. MM/PB(GB)SA calculates the relative free energy of binding for a given macromolecular system using molecular dynamics (MD) simulations [30]. MD simulations are valuable as they depict the structural evolution of a single molecule over time, whereas in a biological system, conformational changes are shown collectively [31].

Since *Warbugia salutaris* compounds display antimycobacterial activity, there are possibilities that it might inhibit mycobacterial QcrB. Inhibition of mycobacterial QcrB by UA and UAA was observed [32]. The Q_P site is the most common site for ligand binding to QcrB, and this is where inhibition is most likely to occur. However, many binding sites in QcrB are being investigated in this study. To solve questions in the field, molecular modelling methods such

2

as molecular docking and MD simulations of *W. salutaris* compounds were applied against mycobacterial QcrB protein. To achieve the aim of this study, we also perform post-MD analyses of the simulated systems using specific methods, primarily MM/GBSA binding free energy calculations. The findings of this study could pave the way for a more focused experimental evaluation of these compounds in the development of new TB drugs targeting the QcrB protein that have minimal side effects and are derived from inexpensive and easily accessible natural resources.

1.2 Aims and objectives of the study

The study has one aim:

1.2.1 To identify *W. salutaris* compounds that possess inhibitory potential against *M. tuberculosis* QcrB protein.

1.2.2 Objectives

To conduct molecular dynamics simulations of UA-, UAA-, Q203- and Lansoprazole-QcrB complexes to:

- Compare the binding affinity of UA and UAA against that of standard drugs Q203 and Lansoprazole on QcrB.

- Determine structural factors that contribute to the inhibitory potential of the compounds.

- Characterise structural dynamics occurring at the protein-ligand interface to comprehend inhibitory mechanisms elicited by the investigated compounds on QcrB.

1.3 Research questions

- Will UA and UAA bind to QcrB protein structure?

- Which binding mode would UA and UAA use?

- What effect would UA, UAA. LSPZ, and Q203 have on the structural dynamics and function of QcrB?

1.4   Novelty and significance of this study

Inhibitors known to target *M. tuberculosis* QcrB are bacteriostatic and notorious for adverse effects on humans. This has motivated a search for potent novel inhibitors derived from natural resources that possess minimum adverse effects. Therapeutics of natural descent are known to possess appreciable adverse effects on humans. In this study, we investigate the inhibitory potential of UA and UAA derived from *W. salutaris* against *M. tuberculosis* QcrB. This was achieved through the application of molecular modelling techniques which include molecular docking, MD simulation, PCA, and MM/PB(GB)SA. The Findings of this study suggest that UA and UAA are more effective compared to LSPZ and Q203. Designing new inhibitors requires an understanding of the binding mechanism of the investigated compounds to the target binding site. UA and UAA exhibited higher binding affinity to QcrB in the porphyrin binding site compared to the known drugs. To our understanding, this is the first instalment of data from the investigation of the inhibitory potential of *W.salutaris* compounds and their mechanism against *M. tuberculosis* QcrB through the usage of *in silico* methods. This study could serve as the basis for further assessment and development of the investigated natural compounds as TB therapeutics targeting QcrB.

1.5   References

1.   Popejoy, M. (2017). The Pandemic Nature of Reemerging Tuberculosis and the Role of Population Migration in its Spread. *MOJ Public Health*, *6*(4), 383–392. https://doi.org/10.15406/mojph.2017.06.00180

2.   World Health Organization. (2020). Global Tuberculosis Control. *Geneva*. https://doi.org/https://www.who.int/publications/i/item/9789240013131

3.   Oni, T., Berkowitz, N., Kubjane, M., Goliath, R., Levitt, N. S., & Wilkinson, R. J. (2017). Trilateral overlap of tuberculosis, diabetes and HIV-1 in a high-burden African setting: Implications for TB control. *European Respiratory Journal*, *50*(1). https://doi.org/10.1183/13993003.00004-2017

4.   Workneh, M.H., Bjune, G.A., Yimer, A. S. (2017). Prevalence and associated factors of tuberculosis and diabetes mellitus comorbidity: A systematic review. *PLoS One*, (12(4)), e0175925.

5.   Getahun, H., Gunneberg, C., Granich, R., Nunn, P. (2010). HIV infectionassociated tuberculosis: the epidemiology and the response. *Clinical infectious diseisease.*, *3*, S201–S207.

6.   Selwyn, P.A., Hartel, D., Lewis, V.A., Schoenbaum, E.E., Vermund, S.H., Klein, R.S., Walker, A.T., Friedland, V. S. (1989). A prospective study of the risk of tuberculosis among intravenous drug users with human immunodeficiency virus infection. *New*

England Journal of Medicine., *320*, 545–550.

7.   World Health Organization. (2010). Multidrug and extensively drug-resistant TB (M/XDR-TB) 2010 Global Report on Surveillance and response. *Geneva, Switzerland*. https://doi.org/https://www.who.int/tb/publications/2019/consolidated-guidelines-drug-resistant-TB-treatment/en/

8.   Ko, Y., & Choi, I. (2016). Putative 3D structure of QcrB from Mycobacterium tuberculosis cytochrome bc1 complex, a novel drug-target for new series of antituberculosis agent Q203. *Bulletin of the Korean Chemical Society*, *37*(5), 725–731. https://doi.org/10.1002/bkcs.10765

9.   Matsoso, L. G., Kana, B. D., Crellin, P. K., Lea-smith, D. J., Pelosi, A., Powell, D., … Mizrahi, V. (2005). Function of the Cytochrome bc 1 - aa 3 Branch of the Respiratory Network in Mycobacteria and Network Adaptation Occurring in Response to Its Disruption. *Journal of Bacteriology*, *187*(18), 6300–6308. https://doi.org/10.1128/JB.187.18.6300

10. Abrahams, K. A., Cox, J. A. G., Spivey, V. L., Loman, N. J., Pallen, M. J., Constantinidou, C., … Besra, G. S. (2012). Identification of Novel Imidazo[1,2-a]pyridine Inhibitors Targeting M. tuberculosis QcrB. *PLoS ONE*, *7*(12). https://doi.org/10.1371/journal.pone.0052951

11. Rybniker, J., Vocat, A., Sala, C., Busso, P., Pojer, F., Benjak, A., & Cole, S. T. (2015). Lansoprazole is an antituberculous prodrug targeting cytochrome bc 1. *Nature Communications*, *6*, 1–8. https://doi.org/10.1038/ncomms8659

12. Kinoshita, Y., Ishimura, N., & Ishihara, S. (2018). Advantages and disadvantages of long-term proton pump inhibitor use. *Journal of Neurogastroenterology and Motility*, *24*(2), 182–196. https://doi.org/10.5056/jnm18001

13. Pandit, R., Singh, P. K., & Kumar, V. (2015). Natural Remedies against Multi-Drug Resistant Mycobacterium tuberculosis. *Journal of Tuberculosis Research*, *03*(04), 171–183. https://doi.org/10.4236/jtr.2015.34024

14. Madikane, V. E., Bhakta, S., Russell, A. J., Campbell, W. E., Claridge, T. D. W., Elisha, B. G., Sim, E. (2007). Inhibition of mycobacterial arylamine N-acetyltransferase contributes to anti-mycobacterial activity of Warburgia salutaris. *Bioorganic and Medicinal Chemistry*, *15*(10), 3579–3586. https://doi.org/10.1016/j.bmc.2007.02.011

15. Khamkar, A., Motghare, V., & Deshpande, R. (2015). Ethnopharmacology—a novel approach for drug discovery. *Indian Journal of Pharmacy and Pharmacology*, *2(4)*, 222–5. https://doi.org/DOI: 10.5958/2393-9087.2015.00007.2

16. Taniguchi, M., Yano, Y., Tada, E., Ikenishi, K., Oi, S., Haraguchi, H., Kubo, I. (1988). Mode of Action of Polygodial, an Antifungal Sesquiterpene Dialdehyde. *Agricultural and Biological Chemistry*, *52*(6), 1409–1414. https://doi.org/10.1080/00021369.1988.10868863

17. Mashimbye, M. J. (1993). Chemical constituents of plants native to Venda. Dissertation, University of Natal.

18. Frum, Y., & Viljoen, A. M. (2006). In vitro 5-lipoxygenase and anti-oxidant activities of South African medicinal plants commonly used topically for skin diseases. *Skin Pharmacology and Physiology*, *19*(6), 329–335. https://doi.org/10.1159/000095253

19. Frum, Y., Viljoen, A. M., & Drewes, S. E. (2005). In vitro 5-lipoxygenase and anti-oxidant activities of Warburgia salutaris and drimane sesquiterpenoids. *South African Journal of Botany*, *71*(3–4), 447–449. https://doi.org/10.1016/S0254-6299(15)30119-8

20. Rabe, T., & Van Staden, J. (2000). Isolation of an antibacterial sesquiterpenoid from Warburgia salutaris. *Journal of Ethnopharmacology*, *73*(1–2), 171–174. https://doi.org/10.1016/S0378-8741(00)00293-2

21. Oloyede, H. O. B., Ajiboye, H. O., Salawu, M. O., & Ajiboye, T. O. (2017). Influence of oxidative stress on the antibacterial activity of betulin, betulinic acid and ursolic acid. *Microbial Pathogenesis*, *111*, 338–344. https://doi.org/10.1016/j.micpath.2017.08.012

22. Fadipe, V. O., Mongalo, N. I., Opoku, A. R., Dikhoba, P. M., & Makhafola, T. J. (2017). Isolation of anti-mycobacterial compounds from Curtisia dentata (Burm.f.) C.A.Sm (Curtisiaceae). *BMC Complementary and Alternative Medicine*, *17*(1), 1–6. https://doi.org/10.1186/s12906-017-1818-9

23. Isa, M. A., Majumdhar, R. S., & Haider, S. (2018). In silico docking and molecular dynamics simulation of 3-dehydroquinate synthase (DHQS) from Mycobacterium tuberculosis. *Journal of Molecular Modelling*, *24*(6), 132.

24. Salo-ahen, O. M. H., Alanko, I., Bhadane, R., Bonvin, A. M. J. J., Honorato, R. V., Hossain, S., … Marimuthu, P. (2021). and Pharmaceutical Development. *Pharmaceutical Development.*, 1–60.

25. De Vivo, M., Masetti, M., Bottegoni, G., & Cavalli, A. (2016). Role of Molecular Dynamics and Related Methods in Drug Discovery. *Journal of Medicinal Chemistry*, *59*(9), 4035–4061. https://doi.org/10.1021/acs.jmedchem.5b01684

26. Xuewei Liu, Danfeng Shi, Shuangyan Zhou, H. L. (n.d.). Molecular dynamics simulations and novel drug discovery. *Expert Opinion on Drug Discovery*, *13*, 23–37. https://doi.org/https://doi.org/10.1080/17460441.2018.1403419

27. Meng, X. Y., Zhang, H. X., Mezei, M., & Cui, M. (2011). Molecular docking: a powerful approach for structure-based drug discovery. *Current Computer Aided Drug Design*, *7*(2), 146–157. https://doi.org/10.2174/157340911795677602

28. Kitchen, D. B., Decornez, H., Furr, J. R., & Bajorath, J. (2004). DOCKING AND SCORING IN VIRTUAL SCREENING FOR DRUG DISCOVERY : METHODS AND APPLICATIONS. *Nature Reviews Drug Discovery.*, *3*(11), 935–49. https://doi.org/10.1038/nrd1549

29. Ramírez, D., & Caballero, J. (2016). Is it reliable to use common molecular docking methods for comparing the binding affinities of enantiomer pairs for their protein target? *International Journal of Molecular Sciences*, *17*(4), 1–15. https://doi.org/10.3390/ijms17040525

30. Kollman, P. A., Massova, I., Reyes, C., Kuhn, B., Huo, S., Chong, L. (2000). Calculating structures and free energies of complex molecules: combiningmolecular mechanics and continuum models. *Accounts of Chemical Research.*, *33*, 889–897. https://doi.org/https://doi.org/10.1021/ar000033j

31. Legge, F. S., Budi, A., Treutlein, H., & Y. I. (2006). Protein fexibility: multiple molecular dynamics simulations of insulin chain B, Biophys. *Chemistry*, *119*, 146–157.

32. Tembe, N., Machaba, K.E., Umar Ndagi., Kumalo, H.M., Mhlongo, N. N. (2022). Ursolic acid as a potential inhibitor of Mycobacterium tuberculosis cytochrome bc1 oxidase-a molecular modelling perspective. *Journal of Molecular modelling*, *28*(2), 35. https://doi.org/doi: 10.1007/s00894-021-04993-w.

2   CHAPTER 2

LITERATURE REVIEW

2.1   Introduction to *Mycobacterium tuberculosis* and new drug targets

Tuberculosis is a life-threatening infectious disease for both humans and animals that is caused by *Mycobacterium* species known as *Mycobacterium tuberculosis* [1]. *M. tuberculosis* was first discovered in 1882 by Robert Koch [2]. *M. tuberculosis* is highly aerobic; requires high oxygen levels for survival. Infection occurs when bacteria enter the lungs and are phagocytosed by macrophages, where they survive the normal antimicrobial phases [3]. Infected macrophages frequently die while attempting to destroy the bacteria, allowing viable bacteria to enter respiratory spaces [4]. Diabetics and HIV co-infected people are particularly vulnerable to TB. Diabetes increases susceptibility to TB via a variety of mechanisms, including hyperglycemia and cellular insulinopenia, both of which have indirect effects on macrophage and lymphocyte function [5]. However, TB can temporarily impair glucose tolerance, which is a risk factor for developing diabetes [6]. Due to the inflammation caused by TB, transient hyperglycemia can occur [7]. HIV co-infected individuals often get infected with TB due to compromised immune systems. HIV promotes the progression of *M. tuberculosis* infection to active TB disease in both newly acquired and latent infections [8] [9]. As HIV infection progresses, CD4/mm3 lymphocytes become depleted, and the immune system becomes less capable of preventing *M. tuberculosis* from spreading throughout the body [10]. A person living with HIV who is also infected with *M. tuberculosis* has a 5–10% annual risk of developing active TB, compared to a 5–10% lifetime risk for someone who is not infected with HIV [11]. Symptoms of TB include fever, fatigue, weight loss, and coughing [12]. According to WHO, the number of active TB cases in 2019 was expected to be 360 000 [13]. In 2019, 14 000 people are expected to become ill with MDR/RR TB in South Africa [13]. This might be due to multi-drug resistance (MDR-

TB) and extensively drug resistance (XDR-TB) which increases at an alarming rate. Failure to complete treatment and prescription of the wrong medication might contribute to MDR-TB [14]. MDR-TB is resistant to isoniazid and rifampicin while XDR-TB is resistant to the main second-line drugs [15].

2.2   Transmission

TB is acquired from other humans through droplet nuclei and the respiratory route. Infectious droplet nuclei develop when people with pulmonary and laryngeal TB shout, cough, or sneeze [16]. When a person inhales TB bacteria-containing droplet nuclei, transmission occurs. These droplet nuclei pass through the mouth or nasal passages and enter the upper respiratory tract [17]; [18]. Thereafter they travel to the bronchi and, finally, the lungs and alveoli [17]. Factors that contribute to TB transmission include duration of exposure, frequency of exposure, and physical proximity to an infectious person. The incubation period may vary from about two to twelve weeks.

2.3   The mycobacterial Electron Transport Chain (ETC)

As an obligate aerobe, *M. tuberculosis* H37Rv respires for energy production via the electron transport chain and oxidative phosphorylation [19]. Mitochondria are essential for respiration because they provide nearly 90% of the ATP required for a normal cell to function. ETC proteins are found in mitochondrial inner membranes, cristae, and prokaryotic cytoplasmic membranes [20]. Cellular respiration is a mechanism in which an energy source (such as sugars, fatty acids, or amino acids) is oxidized while an electron acceptor (such as oxygen, nitrate, sulfur, or sulfate) is simultaneously reduced to provide chemical energy for ATP synthesis. Depending on the source of growth substrates and the supply of terminal electrons acceptors, electrons enter and are shunted through the ETC in several ways [21]. Oxygen is

11

used in the final electron transfer steps under aerobic conditions, and nitrate and fumarate may be used under anaerobic conditions [22].

2.3.1 Nicotinamide adenine dinucleotide (NAD) hydrogen (NADH) dehydrogenases and succinate dehydrogenases (SDH)

In *mycobacteria*, electron transport is induced through the activity of various NADH dehydrogenases and succinate dehydrogenases (SDH), which transfer electrons to menaquinone [23] [24] [25]. The electrons are then transferred to various cytochrome oxidases, which are oxygen-dependent [23] [26] [27]. *M. tuberculosis* H37Rv has two types of NADH dehydrogenases: a proton-translocating type I (NDH-1) and two non-proton-translocating type II (NDH-2) [28]. NDH1 which is required preferentially under aerobic conditions [29] and NDH-2 which favours anaerobic/non-replicating conditions [25] and is primarily used by *Mycobacterium;* have been chemically validated as an *M. tuberculosis* drug target. SDH also known as complex II of the ETC, oxidizes succinate to fumarate in the TCA cycle, thereby donating electrons to the quinone pool [25] [21]. SDH activity is required for metabolic adaptation to hypoxia and ATP synthesis [30], therefore it enables the survival of *M. tuberculosis*. This complex serves as a direct link between the tricarboxylic acid (TCA) cycle and the Oxidative Phosphorylation (OxPhos) pathway, making it essential for bacterial carbon metabolism and respiration [31]. *M. tuberculosis* has two SDH enzymes, Sdh1 and Sdh2, as well as a reversible fumarate reductase that can catalyze both directions of the reaction [31]. Sdh1 is needed for optimal growth under aerobic conditions, according to independent transposon-site hybridization screens in *M. tuberculosis* [32], whereas Sdh2 appears to play a larger role in *M. tuberculosis* growth arrest and dormancy as it transitions from aerobic to hypoxic environments [33].

12

2.3.2 Menaquinone (MK)

MK is an electron carrier involved in the transfer of electrons between ETC components [23]. Electrons from reduced menaquinol may be transferred to either cytochrome *bd*-type menaquinone oxidase or *aa₃*-type cytochrome oxidase (via the cytochrome *bc₁* reductase complex) [27]. MK is made from the precursor chorismate in *M. tuberculosis* through a series of reactions catalyzed by enzymes encoded by the menABCDEFG operon. MenD, MenE, MenB, MenA, and MenG inhibitors with bactericidal activity against non-replicating *M. tuberculosis* have recently been developed. MenF catalyzes the first committed step in chorismate conversion [34], however, it is not considered to be essential due to its deletion which results in growth defects in *M. tuberculosis*. The second step of MK biosynthesis is catalyzed by MenD, a thiamine diphosphate-dependent enzyme. 2-Succinyl-5-enolpyruvyl-6-hydroxy-3-cyclohexene-1-carboxylate is synthesized from 2-oxoglutarate and isochorismate (SEPHCHC) [35]. The MenE gene encodes an o-succinylbenzoate-CoA ligase, which converts o-succinylbenzoate (OSB) to OSB-CoA. In *M. tuberculosis*, it is the fifth step in MK biosynthesis, responsible for the addition of a CoA group via an OSB-AMP intermediate [36]. MenB is a 1,4-dihydroxy-2-naphthoyl-CoA (DHNA-CoA) synthase that catalyzes the conversion of succinylbenzoate-CoA to DHNA-CoA which is involved in the sixth step in MK biosynthesis [37]. MenA is a gene that encodes a 1,4-dihydroxy-2-naphthoate (DHNA)-octaprenyltransferase, which participates in the seventh step of MK biosynthesis. It converts DHNA to demethylmenaquinone (DMK) using a variety of allylic isoprenyl diphosphates as substrates, with at least three isoprene units required [38] [39]. MenG (rv0558) catalyzes the formation of MK by methylating DMK-9 using S-adenosylmethionine and is a final step in MK biosynthesis [40]. The ability to pharmacologically inhibit these enzymes in the MK biosynthesis pathway demonstrates their importance and points to their potential as drug targets. However, the current study focuses more on cytochrome oxidases.

13

2.3.3 Terminal oxidases

Cytochrome bc_1 complex and cytochrome c oxidase also form part of mitochondrial respiratory chain enzymes; respiresome which also forms NADH and SDH. A *beta* subunit of cytochrome bc_1 oxidase plays a key role in TB pathogenesis due to its involvement in bacterial respiration [27]. The respiratory flexibility of the mycobacterium provided by bc_1 cytochrome enables the *Mycobacterium* to survive and replicate within the host cell [41]. The Electrons are transported by the cytochrome bc_1 complex from ubiquinol to cytochrome C, which is important for ATP production and cellular activity across the membrane [42]. The complex is composed of three subunits shown in **Figure 2.1**: Rieske iron-sulfur protein (QcrA), cytochrome B subunit (*QcrB*), and cytochrome C (QcrC)[43] [42] [44]. The N-terminus of QcrA is extended and has three transmembrane helices, QcrC is a diheme c-type cytochrome with two Cys-X-X-Cys-His motifs for covalent heme binding. The QcrB gene is encoded by the β-subunit of the cytochrome bc_1 complex, which acts as menaquinol–cytochrome C oxidoreductase during electron transport. The cytochrome *b* protein forms the hydrophobic core, which also serves as a scaffold for other complex components to interact with [45]. QcrB is made up of eight transmembrane helices and a 120-amino-acid C-terminal extension [46]. According to the Q-cycle model, quinol oxidation occurs at the interface of cytochrome B and the 2Fe–2S cluster carrying domain of the Rieske protein, which forms the catalytic center P on the positively charged membrane side of the enzyme [47]. As a result, QcrB is regarded as an important player in the bc_1 complex's function [48]. Two ubiquinol reactive sites are found in QcrB: the oxidase (Q_P) and the reduction (Q_N) site [49]. The Q_P site for menaquinol (MKH_2) oxidation is close to heme by, whereas the Q_N site for MK reduction is close to heme b_H [50]. Antimycin, a natural product binds on the Q_N site of cytochrome to prevent electron flow from b_H to ubiquinone [51]. The Q_P site is located in the center of an inverted triangle surrounded by

helices [52]. The binding of different inhibitors takes place in the Q_P site since it is the largest site on QcrB [42]. MK binds to the Q_P site in the *bc1* complex [52]. Many inhibitors such as Stigmatellin [53], Q203, and LSPZ also bind to the Q_P site on Cytochrome *b* and block electron transfer. More information on QcrB inhibitors will be discussed in this chapter.

2.3.4   ATP synthase

The F_1F_0 ATP synthase in *M. tuberculosis* consists of two functional domains; a membrane-embedded F_0 unit and an external F_1 domain, which is connected by central and periphery stalks on which F_0 rotates. For the final production of ATP through F_1F_0-ATP synthase, proton motive force (PMF) is an essential aspect [44]. F_1F_0-ATP synthase is involved in the generation of ATP through the use of electrochemical potential energy generated by the proton gradient across the inner membrane of mitochondria [54]. ADP binds successively in the F_1 domains and becomes phosphorylated to form ATP [55]. When intracellular ATP levels are high and the PMF is low, ATP synthase can function as ATPase, hydrolyzing ATP while pumping protons throughout the cytoplasm to re-energize the PMF [56]. However, the ATP synthase in Mycobacteria has been discovered to decrease ATP hydrolysis activity, which has been hypothesized to be an adaptation to conserve ATP under low oxygen tensions [57] [58]. The ATP BEFHAGDC operon in *M. tuberculosis* encodes the F1F0 ATP synthase, which is required for the viability of replicating and non-growing *M. tuberculosis*[43] [59], underlining its importance in ATP generation and sustaining a respiratory electron flow in all metabolic stages [60]. Cell viability is jeopardized by the impairment of processes related to energy metabolism. Since *Mycobacteria* require the more energy-efficient oxidative phosphorylation for growth. The oxidative phosphorylation pathway appears to be a suitable therapeutic target.
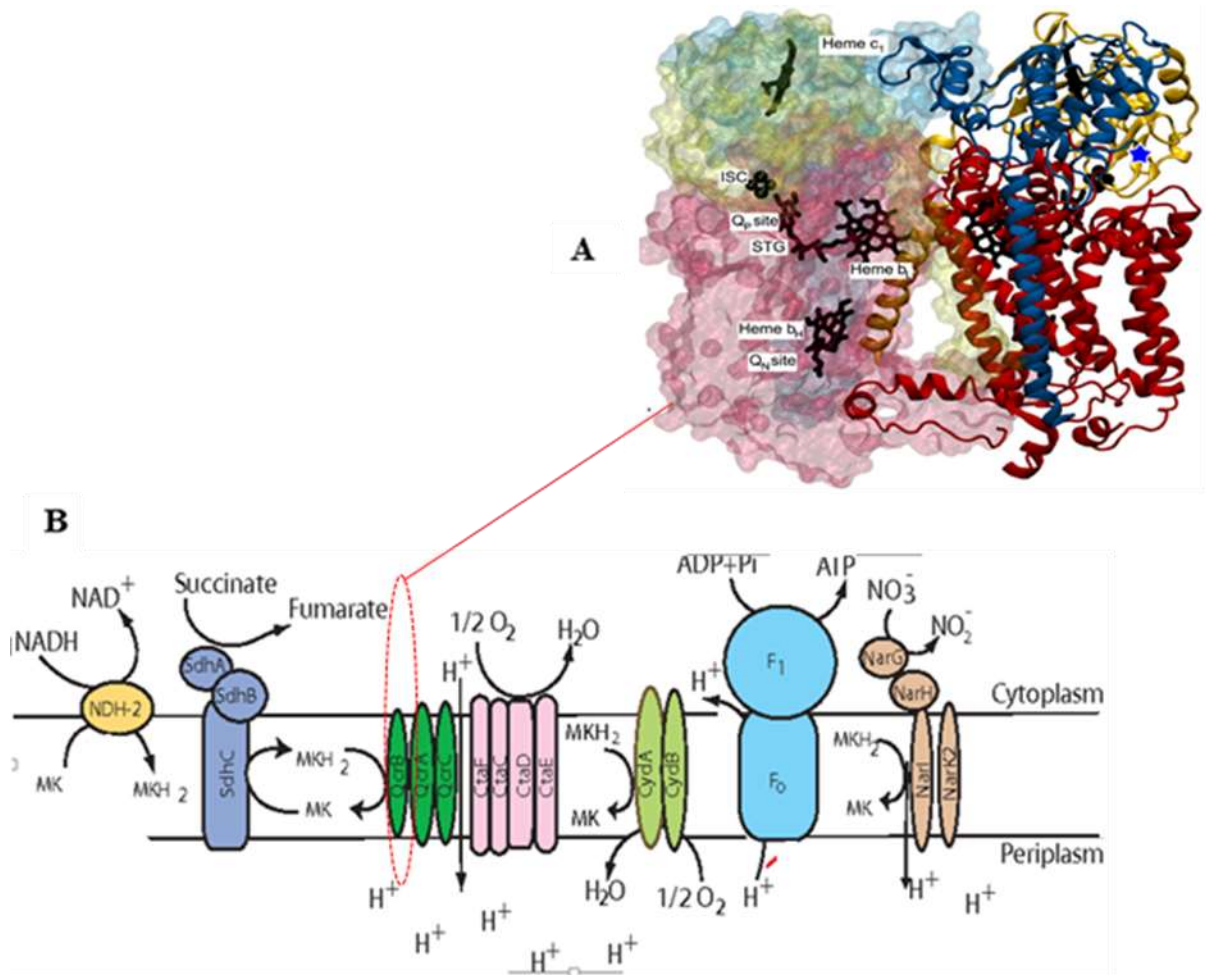
Figure 2. 1: A diagram showing the respiratory chain of mycobacteria **(B)**. NDH-2 (yellow) or succinate (dark blue) can either reduce meloquinone (MK) and cytochrome bc1 (dark green)/ cytochrome aa3 (pink) super complex or cytochrome bd oxidase (light green) can either oxidize MK. The proton motive force is used by ATP synthase (light blue) for ATP generation. Brown shade represents nitrate reductase and transporter system. Small molecules that deplete ATP are shown in red [60]. **(A)** Structure of mycobacteria respiratory complex showing quinol oxidation (Q_P) and reduction site (Q_N) [61].

2.4   Treatment and Drug resistance

A combination of four drugs is used to treat TB for six to nine months [62]. A two-month course of rifampicin, isoniazid, pyrazinamide, and ethambutol, followed by four months of rifampicin and isoniazid, is the first line of treatment for tuberculosis patients [63].

Isoniazid (INH), is commonly used as a first-line treatment and prevention of TB. INH is a prodrug that is activated by catalase-peroxidase KatG [64], resulting in a variety of radicals and adducts that inhibit mycolic acid synthesis which interferes with cell wall synthesis [65]. As a result, a bactericidal effect is produced. INH also interferes with the synthesis or metabolism of DNA, lipids, carbohydrates, and NAD [65]. Resistance to INH is more likely due to mutations and most studies have demonstrated that mutations in INH-resistant are most usually detected in KatG [66].

Rifampicin is an antibacterial agent against many gram-positive cocci; *Mycobacterium spp* and some gram-negative bacteria. Rifampicin is known for inhibition of bacterial DNA-dependent RNA polymerase[63] through drug binding within the DNA/RNA channel's polymerase subunit [67], directly inhibiting the elongating RNA of the 5' end [67]. Resistance develops as a result of mutations that alter the residues of the rifampicin binding site on RNA polymerase [68], resulting in a decreased rifampicin affinity.

Pyrazinamide (PZA) is a critical first-line TB drug that plays a unique role in reducing treatment duration from 9-12 months to 6 months [69]. Pyrazinamide diffuses into the granuloma of *M. tuberculosis*, where it is converted to the active form of pyrazine acid by the TB enzyme pyrazinamidase [70], which is encoded by the pncA gene. Pyrazinoic acid accumulates in bacillus spp under the acidic condition of pH 5 to 6 [70] [71]. Pyrazinoic acid is known to prevent bacteria from synthesizing fatty acids by inhibiting the enzyme Fatty acid synthase (FAS) [72]. It has also been proposed that pyrazinoic acid accumulation disrupts

17

membrane potential and interferes with energy production [73], both of which are required for *M. tuberculosis* survival at an acidic site of infection. The majority of pyrazinamide resistance in *M.tuberculosis* strains is caused by mutations in the pncA gene [74], which encodes a pyrazinamidase that converts pyrazinamide to pyrazinoic acid.

Ethambutol is a bacteriostatic agent that is used in the treatment of pulmonary TB alongside medications like isoniazid, rifampin, and pyrazinamide. Ethambutol penetrates mycobacterial cells. It inhibits arabinosyltransferases once inside the cell, blocking the synthesis of the cell wall components such as arabinogalactin and lipoarabinomannan, as well as cell division [75]. Arabinosyltransferase is encoded by the embCAB operon [76]. The binding site number for mycolic acid is reduced when the concentration of arabinogalactin in the cell wall decreases, resulting in an accumulation of mycolic acid, trehalose monomycolate, and trehalose dimycolate [77].

Ethambutol resistance is caused by mutations in the gene embB, with mutations at location embB306 being the most common in the majority of studies [78]. Mutations in the Rv3806c and Rv3792 genes of the decaprenyl phosphoryl-B-D arabinose (DPA) biosynthetic and utilization pathway, as well as mutations in embC and embB, accumulate [76]. However, these treatments are compromised due to the emergence of MDR-TB and XDR-TB [79]. This is due to the lengthy duration of existing TB therapies with various drugs combination, which frequently causes significant toxicity in patients. Mutations also contribute to resistance. Several drugs have been reported to be effective against *M tuberculosis* ETC. These drugs include bedaquiline (BDQ), Clofazimine (Lamprene), Allylaminomethanone-A -methoxy-2-naphthol, and Biphenyl amide (GSK1733953A), Q203 and LSPZ.

Bedaquiline (BDQ) binds to the ATP synthase c- and ε-subunits by mimicking key residues in the proton transfer chain and preventing the c-rotary subunits from moving during ATP

catalysis [80] [81]. In both actively growing and non-growing bacteria, a fundamental process for survival is disrupted [81]. Due to BDQ uncoupling properties mediated by the H+/K+ antiporter, ATP synthase inhibition results in ATP depletion as well as membrane potential dissipation [82]. Mutations in the gene encoding atpE, specifically the F_0 domain of the ATP synthase enzyme, were found in resistant mutants raised against BDQ [83] [84].

Clofazimine (Lamprene) (CFZ) a hydrophobic rimino-phenazine class antibiotic previously used to treat *Mycobacterium leprae* is now being repurposed for *M. tuberculosis* treatment [85]. NDH-2 is also assumed to be involved in the reduction of CFZ, which results in the generation of reactive oxygen species (ROS) and, as a result, its bactericidal activity against *M. tuberculosis* [86].

Allylaminomethanone-A -methoxy-2-naphthol, an inhibitor that targets menA. It inhibits menA and the growth of *M. tuberculosis* [87]. Some of these compounds are bactericidal against replicating and non-replicating *M. tuberculosis* [88].

Biphenyl amide (GSK1733953A) is involved in MenG inhibition. This drug possesses highly desirable properties for a new antitubercular drug, such as bactericidality against both actively growing and nonreplicating mycobacteria, as well as synergy with several first-line drugs already used in TB treatment [89].

Q203 and LSPZ are identified as imidazopyridine amides (IPA) (Figure 2.2) that target *M. tuberculosis* cytochrome *bc₁* complex by binding to the Q_P site of QcrB. LSPZ is a proton pump inhibitor that is widely used to inhibit gastric acid [90]. The molecules of LSPZ contain a benzimidazole nucleus as well as various branch structures. Proton-pimp inhibitors (PPI) are covalently bound to sulfhydryl (SH) residues of cysteine molecules in the alpha subunit of proton pumps on the secretary canalicular membranes of gastric parietal cells and thereby, inhibiting the secretion of gastric acid [91]. This drug possesses anti-tubercular activity,

however, it does not inhibit $H^+ K^+$-ATPase 9 [92]. Studies have shown that Q203 reduces ATP levels in H37Rv, ATP is required by *M. tuberculosis* for survival [93]. Q203 also enhanced *M. tuberculosis* killing in a macrophage infection model [41]. Both Q203 and LSPZ (Figure 2.2) are bacteriostatic [92]. Q203 and LSPZ do not kill drug-tolerant persisters [93] [44]. This could be due to the adaptation of *M. tuberculosis* to these treatments which leads to resistance and therefore lengthy therapy may be required. Q203 is quite effective when coupled with bedaquiline [35]. This suggests that in the presence of Q203, the alternate terminal bd-type oxidase (cytochrome bd oxidase) can maintain membrane potential and menaquinol oxidation.
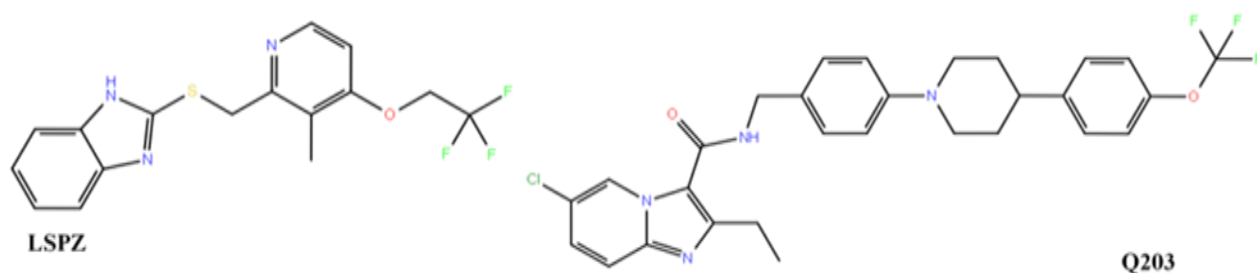
Figure 2. 2: 2D structures of QcrB-inhibitors, LSPZ and Q203.

However, there are adverse effects associated with LSPZ that limit its use. Adverse effects include acute interstitial nephritis, dementia, chronic kidney disease, cerebral ischemic disease, and ischemic cardiac diseases [90]. Q203 does not inhibit oxygen consumption. Inhibiting oxygen consumption can kill *M. tuberculosis* since it depends on oxygen for survival. This limits the clinical applicability of Q203. Therefore, there is a need for alternative treatments against MDR-TB and XDR-TB with reduced side effects. This has stimulated a search for therapeutic compounds with a novel mechanism of action against TB.

2.5   Medicinal plants

Medicinal plants can be defined as any plants that promote health and possess therapeutic properties. Medicinal plants have been used throughout human history for the treatment of various diseases including TB [94]. Almost 75% of approved anti-infective drugs are derived from natural compounds [95]. Due to economic constraints, medicinal plant-based traditional healing has been the major form of medicine used in developing countries to cure diseases and provide primary healthcare [96]. There has been a great interest in the use of medicinal plants and plant-derived compounds in the development and discovery of new effective drugs with low side effects.

The medicinal properties of the plants are attributed to the composition of their secondary metabolites such as terpenoids, phenolic acids, and flavonoids [97]. It is estimated that over 40% of the current drugs in clinical use have their origin in natural products [98]. Medicinal plants that have been found to exhibit anti-tubercular activity include *Clausena anisate* leaves and bark [99]. Methanol extract of Clausena anisate displays anti-mycobacterial properties against *M. tuberculosis* [100]. Leaves of *Haemanthus albiflos* are also used to treat TB [100]. *Artemisa afra* is traditionally used to treat flu and TB, coughs, asthma, and bronchitis [101] while *Cannabis sativ*a leaves are used to treat dry cough [99]. Leaves of *Lippia javanica* [102] and *Carica papaya* [103] have also been reported to exert therapeutic effects against respiratory complications including TB.

2.5.1   Warbugia salutaris

W. salutaris commonly known as pepper bark tree, is an evergreen medium-sized tree that can grow up to 10m in height. This plant is commonly used traditionally to treat symptoms associated with respiratory ailments such as cold, flu, fever, and chest infections. *W. salutaris* extracts and 11a-W-Hydroxycinnamosmolide isolated from the plant exhibited anti-

mycobacterial activity against *M. tuberculosis* H37Rv [104]. Natural compounds isolated from *W. salutaris* shown in Figure 2.3 include warburganal (WB) [105], polygodial (PG) [106], salutarisolide (ST) [107] and muzigadial (MG) [108], which exhibit antifungal and antibacterial activity [109] [110]; ugandensidial (UD), isopolygodial (IPG) and mukaadial (MK) [111] with anti-mycobacterial activity [112]. All-natural compounds, however, exhibit anti-mycobacterial activity. Betulinic acid (BA) and ursolic acid (UA) are naturally occurring triterpenoids with antifungal, antibacterial, antiviral, and anti-HIV properties [113] and anti-tubercular activity [114]. [114]. Ursolic acid acetate (UAA), a derivative of UA, also possesses anti-tubercular activity [114]. UA is also involved in the inhibition of the small heat shock protein of *M. tuberculosis* [115].
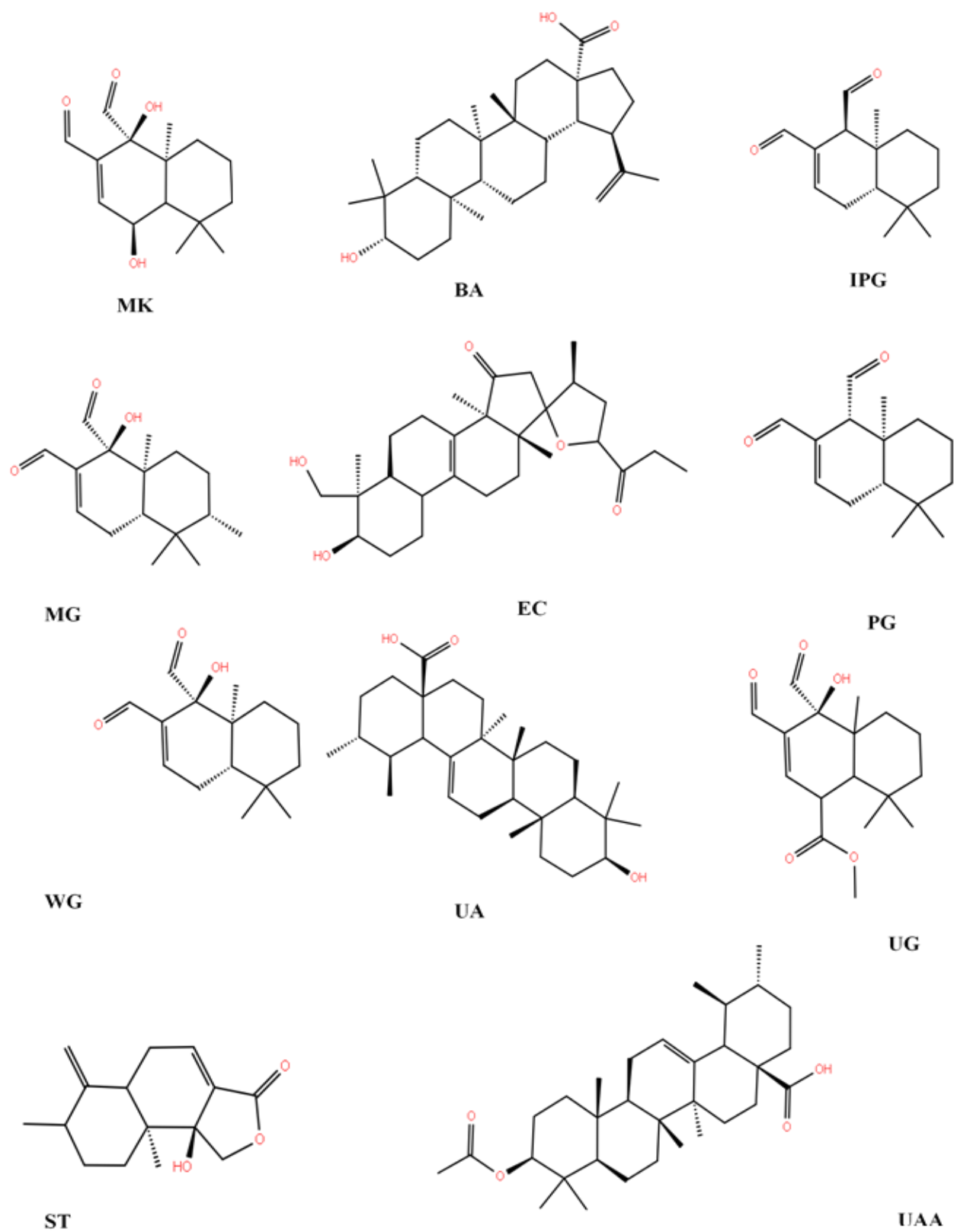
Figure 2. 3: 2D structural formula of compounds from *W.salutaris.*

Given that the majority of medicinal plants have been successfully used to treat TB, natural compounds derived from *W. salutaris* may have inhibitory properties against *M. tub*erculosis cytochrome *bc₁* oxidase, QcrB. In this study, *W.salutaris* compound UA and its derivative UAA, are screened for an inhibitory potential against QcrB. This is accomplished by the usage of *in silico* methods including molecular docking and molecular dynamic simulations. Detailed information about these methods is provided below.

2.6   References

1.   Smith, I. (2003). Mycobacterium tuberculosis pathogenesis and molecular determinants of virulence. *Clinical Microbiology Reviews*, *16*(3), 463–496. https://doi.org/10.1128/CMR.16.3.463-496.2003

2.   Daniel, T. M. (1997). Captain of death: the story of tuberculosis. *University of Rochester Press, Rochester, NY*.

3.   Pieters, J. (2008). Mycobacterium tuberculosis and the Macrophage: Maintaining a Balance. *Cell Host and Microbe*, *3*(6), 399–407. https://doi.org/10.1016/j.chom.2008.05.006

4.   Weiss, G., & Schaible, U. E. (2015). Macrophage defense mechanisms against intracellular bacteria. *Immunological Reviews*, *264*(1), 182–203. https://doi.org/10.1111/imr.12266

5.   Workneh, M.H., Bjune, G.A., Yimer, A. S. (2017). Prevalence and associated factors of tuberculosis and diabetes mellitus comorbidity: A systematic review. *PLoS One*, (12(4)), e0175925.

6.   Pizzol, D., Gennaro, F.D., Chhaganlal, K.D., Fabrizio, C., Monno, L. (2016). Tuberculosis and diabetes: current state and futureperspectives. *Tropical Medicine and International Health*, *6*, 694–702.

7.   Restrepo, B. I. (2016). Diabetes and tuberculosis. *Microbiology Spectrum*, *4(6)*, 1–19.

8.   Getahun, H., Gunneberg, C., Granich, R., Nunn, P. (2010). HIV infectionassociated tuberculosis: the epidemiology and the response. *Clinical infectious disesease.*, *3*, S201–S207.

9.   Selwyn, P.A., Hartel, D., Lewis, V.A., Schoenbaum, E.E., Vermund, S.H., Klein, R.S.,

Walker, A.T., Friedland, V. S. (1989). A prospective study of the risk of tuberculosis among intravenous drug users with human immunodeficiency virus infection. *New England Journal of Medicine.*, *320*, 545–550.

10. Pawlowski, A., Jansson, M., Sköld, M., Rottenberg, M. E., & Källenius, G. (2012). Tuberculosis and HIV co-infection. *PLoS Pathogens*, *8*(2). https://doi.org/10.1371/journal.ppat.1002464

11. Centers for Disease Control and prevention. (2016). Tuberculosis (TB). https://doi.org/https://www.cdc.gov/tb/topic/basics/default.htm

12. Silva, D. R., Muñoz-Torrico, M., Duarte, R., Galvão, T., Bonini, E. H., Arbex, F. F., … Mello, F. C. de Q. (2018). Risk factors for tuberculosis: Diabetes, smoking, alcohol use, and the use of other drugs. *Jornal Brasileiro de Pneumologia*, *44*(2), 145–152. https://doi.org/10.1590/s1806-37562017000000443

13. World Health Organization. (2020). Global Tuberculosis report. https://doi.org/https://www.who.int/publications/i/item/9789240013131

14. World Health Organization. (2010). Multidrug and extensively drug-resistant TB (M/XDR-TB) 2010 Global Report on Surveillance and response. *Geneva, Switzerland*. https://doi.org/https://www.who.int/tb/publications/2019/consolidated-guidelines-drug-resistant-TB-treatment/en/

15. Seung, K. J., Keshavjee, S., & Rich, M. L. (2015). Drug-Resistant Tuberculosis. *Cold Spring Harb Perspectives in Medicine*, *5*(9), 1–20.

16. Nardell, E. A. (2016). Transmission and Institutional Infection Control of Tuberculosis. *Cold Spring Harb Perspectives in Medicine*, *6*(2), 1–12.

17. Ordway, D., Harton, M., Henao-Tamayo, M., Montoya, R., Orme, I.M., Gonzalez-

Juarrero, M. (2006). Enhanced macrophage activity in granulomatous lesions of immune mice challenged with Mycobacterium tuberculosis. *Journal of Immunology*, *17*(8), 4931–9.

18. Orme, I. M. (2014). A new unifying theory of the pathogenesis of tuberculosis. *Tuberculosis (Edinb)*, *94 (1)*, 8–14.

19. Berube, B. J., & Parish, T. (2018). Combinations of respiratory chain inhibitors have enhanced bactericidal activity against mycobacterium tuberculosis. *Antimicrobial Agents and Chemotherapy*, *62*(1), 1–10. https://doi.org/10.1128/AAC.01677-17

20. Kühlbrandt, W. (2015). Structure and function of mitochondrial membrane protein complexes. *BMC Biology*, 1–11. https://doi.org/10.1186/s12915-015-0201-x

21. Cook, G. M., Hards, K., & Vilchèze, C. (2014). NIH Public Access, *2*(3), 1–30. https://doi.org/10.1128/microbiolspec.MGM2-0015-2013.Energetics

22. Bueno, E., Mesa, S., Bedmar, E.J., Richardson, D.J., & Delgado, M. J. (2012). Bacterial Adaptation of Respiration from Oxic to Microoxic. *Antioxidants And Redox Signalling*, *16*(8). https://doi.org/10.1089/ars.2011.4051

23. Kana, B.D., Machowski, E., Schechter, N., Shin, J.T., Rubin, H, Mizrahi, V. (2009). Electron transport and respiration. *Horizon Press, London, United Kingdom.*, 35–64.

24. Unden, G., & Bongaerts, J. (1997). Alternative respiratory pathways of Escherichia coli: Energetics and transcriptional regulation in response to electron acceptors. *Biochimica et Biophysica Acta - Bioenergetics*, *1320*(3), 217–234. https://doi.org/10.1016/S0005-2728(97)00034-0

25. Lancaster, C.R., Kröger, A. (2000). Succinate: quinone oxidoreductases: new insights from X-ray crystal structures. *Biochim. Biophysics*, *1459*, :422– 431.

27

26. Kana, B.D., Weinstein, E.A., Avarbock, D., Dawes, S.S., Rubin, H., Mizrahi, V. (2001). Characterization of the cydAB-encoded cytochrome bd oxidase from Mycobacterium smegmatis. *Journal of Bacteriology.*, *183*, 7076 –7086.

27. Matsoso, L. G., Kana, B. D., Crellin, P. K., Lea-smith, D. J., Pelosi, A., Powell, D., … Mizrahi, V. (2005). Function of the Cytochrome bc 1 - aa 3 Branch of the Respiratory Network in Mycobacteria and Network Adaptation Occurring in Response to Its Disruption. *Journal of Bacteriology*, *187*(18), 6300–6308. https://doi.org/10.1128/JB.187.18.6300

28. Weinstein, E.A.; Yano, T.; Li, L.-S.; Avarbock, D.; Avarbock, A.; Helm, D.; McColm, A.A.; Duncan, K. ., & Lonsdale, J.T.; Rubin, H. (2005). Inhibitors of type II NADH:menaquinone oxidoreductase represent a class of antitubercular drugs. *Proceedings of the National Academy of Sciences of the United States of America*, *102*, 4548–4553.

29. Shi, L., Sohaskey, C.D., Kana, B.D., Dawes, S., North, R.J., M. V, & ML, G. (2005). Changes in energy metabolism of Mycobacterium tuberculosis in mouse lung and under in vitro conditions affecting aerobic respiration. *Proceedings of the National Academy of Sciences of the United States of America*, *102*, 15629 –15634.

30. Black, P. A., Warren, R. M., Louw, G. E., Helden, P. D. Van, Victor, T. C., & Kana, D. (2014). Energy Metabolism and Drug Efflux in Mycobacterium tuberculosis. *Antimicrobial agents Chemotherapy.*, *58*(5), 2491–2503. https://doi.org/10.1128/AAC.02293-13

31. Cook, G.M., Hards, K., Vilchèze, C., Hartman, T., Berney, M. (2014). Energetics of respiration and oxidative phosphorylation in mycobacteria. *Microbiology Spectrum*, *2*, 389–409.

32. Griffin, J.E., Gawronski, J.D., Dejesus, M.A., Ioerger, T.R., Akerley, B.J., Sassetti, C. M. (2011). High-resolution phenotypic profiling defines genes essential for mycobacterial growth and cholesterol catabolism. *PLoS Pathology*, *7*, e1002251.

33. Baek, S.H., Li, A.H., Sassetti, C. M. (2011). Metabolic regulation of mycobacterial growth and antibiotic sensitivity. *PLoS Biology*, *9*, e1001065.

34. Cook, G.M., Hards, K., Dunn, E.,; Heikal, A., Nakatani, Y., Greening, C., Crick, D.C., Fontes, F.L., Pethe, K ., & Hasenoehrl, E. (2017). Oxidative phosphorylation as a target space for tuberculosis: Success, caution, and future directions. *Microbiology Spectrum*, *5*(3), 10.

35. Foo, C. S., & Pethe, K. (2020). Oxidative Phosphorylation — an Update on a New , Essential Target Space for Drug Discovery in Mycobacterium tuberculosis. *Applied Sciences*, *10*(7), 2339.

36. Lu, X., Zhang, H., Tonge, P.J., Tan, D. S. (2008). Mechanism-based inhibitors of MenE, an acyl-CoA synthetase involved in bacterial menaquinone biosynthesis. *Bioorganic and Medicinal Chemistry*, *18*, 5963–5966.

37. Truglio, J.J., Theis, K., Feng, Y., Gajda, R., Machutta, C., Tonge, P.J., Kisker, C. (2003). Crystal structure of Mycobacterium tuberculosis MenB, a key enzyme in vitamin K2 biosynthesis. *Journal of Bioogical Chemistry*, *278*, 42352–42360.

38. Dhiman, R.K., Mahapatra, S., Slayden, R.A., Boyne, M.E., Lenaerts, A., Hinshaw, J.C., Angala, S. K., Chatterjee, D., Biswas, K., Narayanasamy, P., K., & M., Crick, D. C. (2009). Menaquinone synthesis is critical for maintaining mycobacterial viability during exponential growth and recovery from non-replicating persistence. *Molecular Microbiology*, *72*, 85–97.

39.   Debnath, J., Siricilla, S., Wan, B., Crick, D.C., Lenaerts, A.J., Franzblau, S.G., Kurosu, M. (2012). Discovery of selective menaquinone biosynthesis inhibitors against Mycobacterium tuberculosis. *Journal of Medicinal Chemistry*, *55*, 3739–3755.

40.   Goldman, R. C. (2013). Why are membrane targets discovered by phenotypic screens and genome sequencing in Mycobacterium tuberculosis? *Tuberculosis Edinburgh Scotland.*, *93*, 569–588.

41.   Lamprecht, D. A., Finin, P. M., Rahman, M. A., Cumming, B. M., Russell, S. L., Jonnala, S. R., … Steyn, Adrie, J. C. (2016). Turning the respiratory flexibility of Mycobacterium tuberculosis against itself. *Nature Communications*, *7*, 1–14. https://doi.org/10.1038/ncomms12393

42.   Ko, Y., & Choi, I. (2016). Putative 3D structure of QcrB from Mycobacterium tuberculosis cytochrome bc1 complex, a novel drug-target for new series of antituberculosis agent Q203. *Bulletin of the Korean Chemical Society*, *37*(5), 725–731. https://doi.org/10.1002/bkcs.10765

43.   Sassetti, C. M., Boyd, D. H., & Rubin, E. J. (2003). Genes required for mycobacterial growth defined by high density mutagenesis. *Molecular Microbiology*, *48*(1), 77–84. https://doi.org/10.1046/j.1365-2958.2003.03425.x

44.   Iqbal, I. K., Bajeli, S., Akela, A. K., & Kumar, A. (2018). Bioenergetics of mycobacterium: An emerging landscape for drug discovery. *Pathogens*, *7*(1). https://doi.org/10.3390/pathogens7010024

45.   Crofts, A.R., Berry, E. A. (1998). Structure and function of the cytochrome bc1 complex of mitochondria and photosynthetic bacteria. *Current Opinion in Structural Biology*, *8*, 501–509.

46.   Niebisch, A., & Bott, M. (2001). Molecular analysis of the cytochrome bc1-aa3 branch of the Corynebacterium glutamicum respiratory chain containing an unusual diheme cytochrome c1. *Archives of Microbiology*, *175*(4), 282–294. https://doi.org/10.1007/s002030100262

47.   Schagger, H., Cramer, W. A., & Vonjagow, G. (1994). Analysis of Molecular Masses and Oligomeric states of Protein Complexes by Blue Native Electrophoresis and Isolation of Membrane Protein Complexes by Two-Dimensional Native Electrophoresis. *Analytical Biochemistry*, *217*(2), 220–230. https://doi.org/DOI: 10.1006/abio.1994.1112

48.   Gao, X., & Wen, X. et al. (2002). The Crystal Structure of Mitochondrial Cytochrome bc1 in Complex with Famoxadone : The Role of Aromatic - Aromatic Interaction in Inhibition. *Biochemistry*, 11692–11702. https://doi.org/DOI: 10.1021/bi026252p

49.   Crofts, A. R., Guergova-Kuras, M., Kuras, R., Ugulava, N., Li, J., & Hong, S. (2000). Proton-coupled electron transfer at the Q(o) site: What type of mechanism can account for the high activation barrier? *Biochimica et Biophysica Acta - Bioenergetics*, *1459*(2–3), 456–466. https://doi.org/10.1016/S0005-2728(00)00184-5

50.   Xia, D., Esser, L., Tang, W.K., Zhou, F., Zhou, Y., Yu, L., Yu, C. A. (2013). Structural analysis of cytochrome bc1 complexes: implications to the mechanism of function. *Biochim Biophys Acta*, *1827*, 1278–1294.

51.   Xia D, et al. (1997). Crystal structure of the cytochrome bc1 complex from bovine heart mitochndria. *Science*, *277*, 60–66.

52.   Zhou, S., Wang, W., Zhang, Y., et al. (2021). Structure of Mycobacterium tuberculosis cytochrome bcc in complex with Q203 and TB47, two anti-TB drug candidates. *Structural Biology and Molecular Biophysics*, *10*, e69418. https://doi.org/. doi:

53.   Von Jagow, G., Ljungdahl, P.O., Graf, P., Ohnishi, T., Trumpower, B. (1984). An inhibitor of mitochondrial respiration which binds to cytochrome b and displaces quinone from the iron-sulfur protein of the cytochrome bc1 complex. *Journal of Biological Chemistry.*, *259*, 6318–6326.

54.   Feniouk, B.A., Suzuki, T., Yoshida, M. (2007). Regulatory interplay between proton motive force, ADP, phosphate, and subunit epsilon in bacterial ATP synthase. J. *Journal of Biological Chemistry*, *282*, 764–772.

55.   Walker, J. E. (2013). The ATP synthase: The understood, the uncertain and the unknown. *Biochemistry Society Transactions*, *41*, 1–16.

56.   von Ballmoos, C., Cook, G.M., Dimroth, P. (2008). Unique rotary atp synthase and its biological diversity. *Annual Review of Biophysics*, *37*, 43–64.

57.   Higashi, T., Kalra, V.K., Lee, S.H., Bogin, E., Brodie, A. F. (1975). Energy-transducing membrane-bound coupling factor-ATPase from Mycobacterium phlei. I. Purification, homogeneity, and properties. *Journal of Biological ChemistryChemistry*, *250*, 6541–6548.

58.   Lu, P., Lill, H., Bald, D. (2014). ATP synthase in mycobacteria: Special features and implications for a function as drug target. *Biochimaet Biophysica. Acta BBA-Bioenergetics*, *1837*, 1208–1218.

59.   DeJesus, M.A., Gerrick, E.R., Xu, W., Park, S.W., Long, J.E., Boutte, C.C., Rubin, E.J., Schnappinger, D., Ehrt, S., & Fortune, S. M. (2017). Comprehensive essentiality analysis of the mycobacterium tuberculosis genome via saturating transposon mutagenesis. *Journal of Microbiology & Biology Education*, *8*, e02133-16.

60. Bald, D., Koul, A. (2010). Respiratory ATP synthesis: The new generation of mycobacterial drug targets? *FEMS Microbiology Letters.*, *308*, 1–7.

61. Gong, H., Li, J., Xu, A., Ji, W., Gao, R., Wang, S., Tian, C. Li, J., Rao, W. et al. (2018). Cryo-EM reveals an electron transfer path in a Mycobacterial respiratory supercomplex. *Science*, *362*(6418).

62. World Health Organization. (2010). World Health Organization, Guidelines for Treatment of Tuberculosis. *4th edition*. https://doi.org/WHO/HTM/TB/2009.420

63. Centers for Disease Control and prevention. (2003). Treatment of tuberculosis. https://doi.org/https://www.cdc.gov/mmwr/preview/mmwrhtml/rr5211a1.htm

64. Unissa, A. N., Subbian, S., Hanna, L. E., & Selvakumar, N. (2016). Overview on mechanisms of isoniazid action and resistance in Mycobacterium tuberculosis. *Infection, Genetics and Evolution*, *45*(1), 474–492. https://doi.org/10.1016/j.meegid.2016.09.004

65. Timmins, G. S., & Deretic, V. (2006). Mechanisms of action of isoniazid. *Molecular Microbiology*, *62*(5), 1220–1227. https://doi.org/10.1111/j.1365-2958.2006.05467.x

66. Zhang, Y., Heym, B., Allen, B., Young, D., and Cole, S. (1992). The catalase-peroxidase gene and isoniazid resistance of Mycobacterium tuberculosis. *Nature*, *358*, 591–593.

67. Campbell, E.A., Korzheva, N., Mustaev, A., Murakami, K., Nair, S., Goldfarb, A., Darst, S. A. (2001). "Structural mechanism for rifampicin inhibition of bacterial rna polymerase." *Cell*, *104 (6)*, 901–12.

68. Molodtsov, V., Scharf, N.T., Stefan, M.A., Garcia, G.A., & Murakami, K. S. (2018). Structural basis for Rifamycin resistance of bacterial RNA polymerase by the three most clinically important RpoB mutations found in Mycobacterium tuberculosis. *Molecular Microbiology*, *103*(6), 1034–1045. https://doi.org/10.1111/mmi.13606.Structural

69. Fox, W., Ellard, G.A., Mitchison, D. A. (1999). Studies on the treatment of tuberculosis undertaken by the British Medical Research Council tuberculosis units, 1946–1986, with relevant subsequent publications. *International Journal of Tuberculosis Lung Disease*, *3*, S231–279.

70. Whitfield, M.G., Soeters, H.M., Warren, R. M., Talita, Y., Sampson, S.L., Streicher, E.M., Helden, P.D., Van, R., Van, A. (2015). "A Global Perspective on Pyrazinamide Resistance: Systematic Review and Meta-Analysis." *PLOS ONE*, *10 (7)*, e0133869.

71. Zhang, Y., Mitchison, D. (2003). "The curious characteristics of pyrazinamide: a review." *International Journal of Tuberculosis Lung Disease*, *7 (1)*, 6–21.

72. Zimhony, O., Cox, J.S., Welch, J.T., Vilchèze, C., Jacobs, W. R. (2000). "Pyrazinamide inhibits the eukaryotic-like fatty acid synthetase I (FASI) of Mycobacterium tuberculosis." *Nature Medicine.*, *6 (9)*, 1043–47.

73. Zhang, Y., Wade, M.M., Scorpio, A., Zhang, H., Sun, Z. (2003). Mode of action of pyrazinamide: disruption of Mycobacterium tuberculosis membrane transport and energetics by pyrazinoic acid. *Journal of Antimicrobial Chemotherapy*, *52*, 790–795.

74. Zhang, Y., Shi, W., Zhang, W., & Mitchison, D. (2014). Mechanisms of Pyrazinamide Action and Resistance The History: The Unusual Discovery and the Roller Coaster of PZA. *Microbiol Spectr*, *2*(4), 1–12. https://doi.org/10.1128/microbiolspec.MGM2-0023-2013.Mechanisms

75. Palomino, J.C., Martin, A. (2014). Drug Resistance Mechanisms in Mycobacterium tuberculosis. *Antibiotics (Basel).*, *3(3)*, 317–40.

76. Safi, H., Lingaraju, S., Amin, A., Kim, S., Jones, M., Holmes, M., McNeil, M., Peterson, S.N., Chatterjee, D., Fleischmann, R., & Alland, D. (2013). Evolution of high-level

ethambutol-resistant tuberculosis through interacting mutations in decaprenylphosphoryl-β-d-arabinose biosynthetic and utilization pathway genes. *Nature genetics*, *45*, 1190–1197.

77. North, E.J., & Jackson, M. (2014). New Approaches to Target the Mycolic Acid Biosynthesis Pathway for the Development of Tuberculosis Therapeutics. *Current Pharmaceutical Design.*, *20(27)*, 4357–4378.

78. Zhang, Y. Y. (2015). Mechanisms of drug resistance in Mycobacterium tuberculosis: update 2015. *International Journal of Tuberculosis Lung Disease*, *19(11)*, 1276–89.

79. World Health Organization. (2018). What is multidrug-resistant tuberculosis (MDR-TB) and how do we control it? https://doi.org/https://www.who.int/news-room/questions-and-answers/item/tuberculosis-multidrug-resistant-tuberculosis-(mdr-tb).

80. Biukovic, G., Basak, S., Manimekalai, M.S., Rishikesan, S., Roessle, M.D., Rao, S.P, H. C. (2013). Variations of subunit epsilon of the Mycobacterium tuberculosis F1F0 ATP synthase and a novel model for mechanism of action of the TB drug TMC207. *Antimicrobial Agents Chemotherapy*, *57*, 168–176.

81. Koul, A., Vranckx, L., Dendouga, N., Balemans, W., den Wyngaert, I.V., Vergauwen, K., Göhlmann, H. W. H., Willebrords, R., & Poncelet, A. G. (2008). Diarylquinolines are bactericidal for dormant mycobacteria as a result of disturbed ATP homeostasis. *Journal of Biological Chemistry.*, *283*, 25273–25280.

82. Hards, K., McMillan, D.G.G., Schurig-Briccio, L.A., Gennis, R.B., Lill, H,; Bald, D., Cook, G. M. (2018). Ionophoric e ects of the antitubercular drug bedaquiline. *Proceedings of the National Academy of Sciences of the United States of America*, *115*, 7326–7331.

83. Xu, J., Wang, B., Hu, M., Huo, F.,; Guo, S., Jing, W., Nuermberger, E.,; Lu, Y. (2017). Primary clofazimine and bedaquiline resistance among isolates from patients with multidrug-resistant tuberculosis. *Antimicrobial Agents Chemotherapy.*, *61*, e00239-17.

84. Villellas, C., Coeck, N., Meehan, C.J., Lounis, N., de Jong, B., Rigouts, L., Andries, K. (2017). Unexpected high prevalence of resistance-associated Rv0678 variants in MDR-TB patients without documented prior use of clofazimine or bedaquiline. *Journal of Antimicrobial Chemotherapy*, *72*, 684–690.

85. Yawalkar, S., McDougall, A., Languillon, J., Ghosh, S., Hajra, S. (1982). Once-monthly rifampicin plus daily dapsone in initial treatment of lepromatous leprosy. *Lancet*, *319 (8283)*, 1199–1202.

86. Yano, T., Kassovska-Bratinova, S., Teh, J.S., Winkler, J., Sullivan, K., Isaacs, A., Schechter, N.M., Rubin, H. (2011). Reduction of clofazimine by mycobacterial type 2 NADH: Quinone oxidoreductase: A pathway for the generation of bactericidal levels of reactive oxygen species. *Journal of Biology and Chemistry*, *286*, 10276–10287.

87. Kurosu, M., and Dean, C. C. (2009). MenA Is a Promising Drug Target for Developing Novel Lead Molecules to Combat Mycobacterium tuberculosis. *Medicinal Chemistry*, *5(2)*, 197–207.

88. Berube, B.J., Russell, D., Castro, L., Choi, S., Narayanasamy, P., Parish, T. (2019). Novel mena inhibitors are bactericidal against mycobacterium tuberculosis and synergize with electron transport chain inhibitors. *Antimicrobial Agents of Chemotherapy.*, *63*, e02661-18.

89. Sukheja, P., Kumar, P., Mittal, N., Li, S., Singleton, E., Russo, R., Perryman, A.L., Shrestha, R., Awasthi, D., Husain, S., Soteropoulos, P., Brukh, R., Connell, N., Freundlich, J.S., D. A. (2017). A Novel Small-Molecule Inhibitor of theMycobacterium

36

tuberculosisDemethylmenaquinoneMethyltransferase MenG Is Bactericidalto Both Growing and NutritionallyDeprived Persister cells. *AMERICAN SOCIETY FOR MICROBIOLOGY*, *8*(1), e02022-16.

90.   Kinoshita, Y., Ishimura, N., & Ishihara, S. (2018). Advantages and disadvantages of long-term proton pump inhibitor use. *Journal of Neurogastroenterology and Motility*, *24*(2), 182–196. https://doi.org/10.5056/jnm18001

91.   Shin, J. M., Sachs, G., Cho, Y., & Garst, M. (2009). 1-Arylsulfonyl-2-(Pyridylmethylsulfinyl) Benzimidazoles as New Proton Pump Inhibitor Prodrugs. *Molecul;es*, 5247–5280. https://doi.org/10.3390/molecules14125247

92.   Rybniker, J., Vocat, A., Sala, C., Busso, P., Pojer, F., Benjak, A., & Cole, S. T. (2015). Lansoprazole is an antituberculous prodrug targeting cytochrome bc 1. *Nature Communications*, *6*, 1–8. https://doi.org/10.1038/ncomms8659

93.   Kalia, N. P., Hasenoehrl, E. J., Rahman, N. B. A., Koh, V. H., Ang, M. L. T., Sajorda, D. R., … Pethe, K. (2017). Exploiting the synthetic lethality between terminal respiratory oxidases to kill Mycobacterium tuberculosis and clear host infection. *Proceedings of the National Academy of Sciences of the United States of America*, *114*(28), 7426–7431. https://doi.org/10.1073/pnas.1706139114

94.   Pandit, R., Singh, P. K., & Kumar, V. (2015). Natural Remedies against Multi-Drug Resistant Mycobacterium tuberculosis. *Journal of Tuberculosis Research*, *03*(04), 171–183. https://doi.org/10.4236/jtr.2015.34024

95.   Pereira, F. (2019). Have marine natural product drug discovery efforts been productive and how can we improve their efficiency? *Expert Opinion on Drug Discovery*, *14*(8), 717–722. https://doi.org/10.1080/17460441.2019.1604675

96.   Aziz, M. A., Adnan, M., Khan, A. H., Shahat, A. A., Al-said, M. S., & Ullah, R. (2018). Traditional uses of medicinal plants practiced by the indigenous communities at Mohmand Agency , FATA , Pakistan. *Journal of Ethnobiology and Ethnomedicine*, 1–16. https://doi.org/10.1186/s13002-017-0204-5

97.   Tungmunnithum, D., Thongboonyou, A., & Pholboon, A. (2018). Flavonoids and Other Phenolic Compounds from Medicinal Plants for Pharmaceutical and Medical Aspects : An Overview. *Medicines*. https://doi.org/10.3390/medicines5030093

98.   Babalola, I. T., & Shode, F. O. (2013). Ubiquitous Ursolic Acid : A Potential Pentacyclic Triterpene Natural Product . *Journal of Ethnobiology and Ethnomedicine*, *2*(2), 214–222.

99.   Hutchings, A., Scott, A.H., Lewis, G., Cunningham, A. (1996). Zulu Medicinal Plants. Natal University Press, Pietermaritzburg. *American Chemical Society and American Society of Pharmacognosy*, *60*, 9–955.

100.   Lawal, I.O., Grierson, D.S., Alfolayan, A. J. (2014). Phytotherapeutic Information on Plants Used for the Treatment of Tuberculosis in Eastern Cape Province, South Africa. *Evidence-Based Complementary and Alternative Medicine*, 11.

101.   Van Wyk, B.E., Gericke, N. (2000). People's Plants: A Guide to Useful Plantsof Southern Africa. *Briza Publications, Pretoria*, *352*.

102.   Watt, J.M., Breyer-Brandwijk, M. G. (1962). The Medicinal plants and Poisonous Plants of Southern and Eastern Africa. *2nd Edition, E. and S. Livingstone Ltd., Edinburgh.*

103.   Van Wyk, B.E. van Oudshoorn, B. and Gericke, N. (2009). Medicinal plants of South Africa. *Journal of the South African Veterinary Association, 2nd edition.*, Pretoria, South Africa pp188. https://doi.org/DOI: 10.4102/jsava.v81i3.145

104. Madikane, V. E., Bhakta, S., Russell, A. J., Campbell, W. E., Claridge, T. D. W., Elisha, B. G., Sim, E. (2007). Inhibition of mycobacterial arylamine N-acetyltransferase contributes to anti-mycobacterial activity of Warburgia salutaris. *Bioorganic and Medicinal Chemistry*, *15*(10), 3579–3586. https://doi.org/10.1016/j.bmc.2007.02.011

105. Khamkar, A., Motghare, V., & Deshpande, R. (2015). Ethnopharmacology—a novel approach for drug discovery. *Indian Journal of Pharmacy and Pharmacology*, *2(4)*, 222–5. https://doi.org/DOI: 10.5958/2393-9087.2015.00007.2

106. Taniguchi, M., Yano, Y., Tada, E., Ikenishi, K., Oi, S., Haraguchi, H., Kubo, I. (1988). Mode of Action of Polygodial, an Antifungal Sesquiterpene Dialdehyde. *Agricultural and Biological Chemistry*, *52*(6), 1409–1414. https://doi.org/10.1080/00021369.1988.10868863

107. Frum, Y., & Viljoen, A. M. (2006). In vitro 5-lipoxygenase and anti-oxidant activities of South African medicinal plants commonly used topically for skin diseases. *Skin Pharmacology and Physiology*, *19*(6), 329–335. https://doi.org/10.1159/000095253

108. Frum, Y., Viljoen, A. M., & Drewes, S. E. (2005). In vitro 5-lipoxygenase and anti-oxidant activities of Warburgia salutaris and drimane sesquiterpenoids. *South African Journal of Botany*, *71*(3–4), 447–449. https://doi.org/10.1016/S0254-6299(15)30119-8

109. Mahmoud, I., Kinghorn, A., Cordell, A., & Farnsworth, N. (1980). Potential anticancer agents. XVI. Isolation of bicyclofarnesane sesquiterpenoids from Capsicodendron dinisii. *Mahmoud, I., Kinghorn, A., Cordell, A., & Farnsworth, N.*, *43*(Suppl 3), 365–71.

110. Nakanishi, K., & Kubo, I. (1978). ChemInform Abstract: STUDIES ON WARBURGANAL, MUZIGADIAL AND RELATED COMPOUNDS. *Chemischer Informationsdienst*, *9*(14), 28–31. https://doi.org/10.1002/chin.197814354

111. Rabe, T., & Van Staden, J. (2000). Isolation of an antibacterial sesquiterpenoid from Warburgia salutaris. *Journal of Ethnopharmacology*, *73*(1–2), 171–174. https://doi.org/10.1016/S0378-8741(00)00293-2

112. Mashimbye, M. J. (1999). A drimane sesquiterpinoid lactone from Warburgia salutaris. *Phytochemistry.*, *51*, 435–8.

113. Oloyede, H. O. B., Ajiboye, H. O., Salawu, M. O., & Ajiboye, T. O. (2017). Influence of oxidative stress on the antibacterial activity of betulin, betulinic acid and ursolic acid. *Microbial Pathogenesis*, *111*, 338–344. https://doi.org/10.1016/j.micpath.2017.08.012

114. Fadipe, V. O., Mongalo, N. I., Opoku, A. R., Dikhoba, P. M., & Makhafola, T. J. (2017). Isolation of anti-mycobacterial compounds from Curtisia dentata (Burm.f.) C.A.Sm (Curtisiaceae). *BMC Complementary and Alternative Medicine*, *17*(1), 1–6. https://doi.org/10.1186/s12906-017-1818-9

115. Jee, B., Kumar, S., Yadav, R., Singh, Y., Kumar, A., Sharma, N. (2018). Ursolic acid and carvacrol may be potential inhibitors of dormancy protein small shock protein16.3 of Mycobacterium tuberculosis. *Journal of Biomolecular Structure and Dynamics*, *36*(13), 3434–3443. https://doi.org/doi:10.1080/07391102.2017.1389305.)

3   CHAPTER 3

RESULTS AND DISCUSSION

Published manuscript

Ursolic acid as a potential inhibitor of *Mycobacterium tuberculosis* cytochrome *bc1* oxidase ─ a molecular modelling perspective

Ntombikayise Tembe[1], Kgothatso E. Machaba[1], Umar Ndagi[2], Hezekiel M. Kumalo[1] and Ndumiso N. Mhlongo[1*]

[1]School of Laboratory Medicine and Medical Sciences, University of KwaZulu-Natal, Durban 4001, South Africa

[2]Africa Centre of Excellence for Mycotoxin and Food Safety, Federal University of Technology, Minna

* Corresponding author: Ndumiso N. Mhlongo

Email: MhlongoN4@ukzn.ac.za

Telephone: +2731 260 2428, Fax: +2731 260 7792

Abstract

The escalating burden of tuberculosis disease and drastic effects of current medicine has stimulated a search for alternative drugs. A medicinal plant *Warburgia salutaris* has been reported to possess inhibitory properties against *M.tuberculosis*. In this study we apply computational methods to investigate the probability of *W. salutaris* compounds as potential inhibitors of *M. tuberculosis* QcrB protein. We performed Molecular Docking, Molecular Dynamics simulations, Radius of Gyration, Principal Component Analysis (PCA), and Molecular Mechanics-Generalized Born Surface Area (MM/GBSA) binding free energy calculations in explicit solvent to achieve our objective. The results suggested that ursolic acid (UA) and ursolic acid acetate (UAA) could serve as preferred potential inhibitors of mycobacterial QcrB compared to lansoprazole sulphide (LSPZ) and telacebec (Q203) .UA and UAA have a higher binding affinity to QcrB compared to LSPZ and Q203 drugs. UA binding affinity is attributed to hydrogen bond formation with Val120, Arg364 and Arg366, and largely resonated from van der Waals forces resulting from UA interactions with hydrophobic amino acids in its vicinity. UAA binds to the porphyrin ring binding site with higher binding affinity compared to LSPZ. The binding affinity results primarily from van der Waals forces between UAA and hydrophobic residues of QcrB in the porphyrin ring binding site where UAA binds competitively. UA and UAA formed stable complexes with the protein with reduced overall residue mobility, consequently supporting the magnitude of binding affinity of the respective ligands. UAA could potentially compete with the porphyrin ring for the binding site and deprive the mycobacterial cell from oxygen, consequently disturbing mycobacterial oxygen-

dependent metabolic processes. Therefore, discovery of a compound that competes with porphyrin ring for the binding site may be useful in QcrB pharmocological studies. UA proved to be a superior compound, although its estimated toxicity profile revealed UA to be hepatotoxic within acceptable parameters. Although preliminary findings of this report still warrant experimental validation, they could serve as a baseline for the development of new anti-tubercular drugs from natural resources that target QcrB.

Keywords: *W. salutaris*; *M. tuberculosis*; QcrB; molecular dynamics simulation; MM/GBSA; PCA; potential inhibitor

3.1 Introduction

Mycobacterium tuberculosis, a causative agent of tuberculosis (TB) disease, remains one of the leading cause of death worldwide since ancient times [1]. TB remains to be a major global public health issue with 10 million cases of TB infection and 1.57 million TB-related deaths reported worldwide, in 2017 [2]. Nevertheless, TB can be treated by a mixture of four drugs for a period of 6 to 9 months. The first line drugs administered to TB patients include a combination of rifampicin, isoniazid, pyrazinamide and ethambutol for 2 months followed by rifampicin and isoniazid for 4 months. Hence, inappropriate use or failure to complete the full course of treatment lead to multi-drug resistance (MDR) and extensively drug-resistance (XDR) strains of *M. tuberculosis* [3]. For these reason, effective drugs against simplify treatment of drug-sensitive TB and drug-resistant TB are in demand.

M. tuberculosis H37Rv is an obligate aerobe, which means it uses electron transport chain and oxidative phosphorylation to generate energy through respiration [4]. A *beta* subunit of cytochrome bc_1 oxidase plays a crucial role in the pathogenesis of TB since it is involved in bacterial respiration [5]. The respiratory flexibility of the mycobacterium by bc_1 cytochrome allows the mycobacterium to survive and replicate inside the host cell [6].Cytochrome bc_1 complex transport electrons across the membrane from ubiquinol to cytochrome C which is responsible for ATP synthesis and cellular activity [7] [8][9]. The complex is constitute of three subunits: Rieske iron-sulphur protein (QcrA), cytochrome B subunit (QcrB) and cytochrome C (QcrC) [10]; [7]; [11]. QcrA contain an extended N-terminus with three transmembrane helices. QcrB contains eight transmembrane helices, a C-terminal extension of about 120

44

amino acids [12]. According to Q-cycle model, oxidation of quinol molecules occurs at the interface of cytochrome b and the 2Fe–2S cluster carrying domain of the Rieske protein [13]. This forms the catalytic centre P at the positively charged membrane side of the enzyme [14] . Hence, QcrB is regarded as an important player in the function of bc_1 complex [15]. QcrB contains two ubiquinol reactive sites: the oxidase (Q_P) and the reduction (Q_N) site [16][13]. The binding of various inhibitors commonly occur in the Q_P site, as it is the largest site on QcrB [7].

 FDA-approved drugs such as imidazo-pyrimidine amide (Q203) and lansoprazole (LSPZ) (Figure 3.1) display anti-tubercular activity against *M. tuberculosis* by targeting a *beta* subunit of the cytochrome *bc₁* complex. Cytochrome *bc₁* oxidase is encoded by the gene QcrB and also triggers rapid ATP depletion [17]; [7]. Both Q203 and LSPZ are bacteriostatic [18], hence they do not kill drug-tolerant persisters [19]; [11]. Inhibiting oxygen consumption can kill *M. tuberculosis* since it depends on it for survival [19]. Q203 does not inhibit oxygen consumption of the mycobacterium. Moreover, these drugs are associated with adverse side effects such as dementia, chronic kidney disease and ischemic cardiac diseases [20]. For this reason, novel TB drugs are needed to provide alternative therapy with less side effects, and compounds from natural resources are proclaimed of such character.
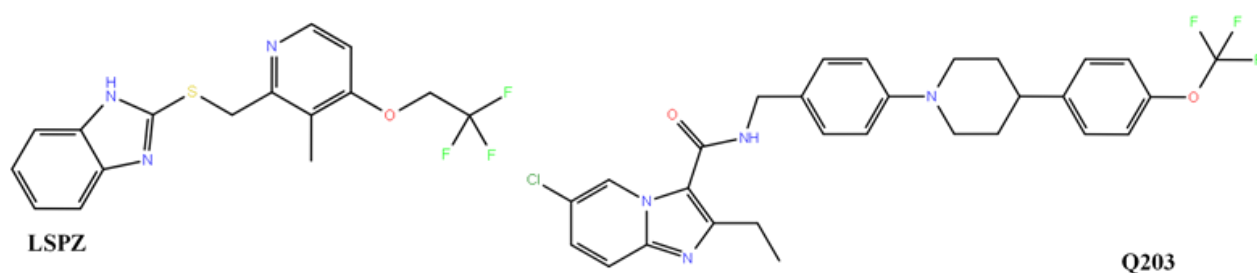

Figure 3.1: Structures of known QcrB-inhibitors, LSPZ and Q203.

Medicinal plants have been widely used anciently to efficiently treat various threatening diseases including TB[21]. *Warburgia salutaris* leaves, roots and bark are traditionally used to treat abdominal pain, ulcers, influenza, malaria [22], respiratory complaints and tuberculosis [23]. *W. salutaris* extract exhibited antimycobacterial activity against *Mtb* H37Rv [24]; however its mode of inhibition has not been fully explained.

Compounds isolated from *W. salutaris* include warburganal (WB) [25], polygodial (PG) [26], salutarisolide (ST) [27] [28] and muzigadial (MG) [29], which exhibit antifungal and antibacterial activity [30] [31]; ugandensidial (UD), isopolygodial (IPG) and mukaadial (MK) [32] with anti-mycobacterial activity [33] (Figure 3.2). Betulinic acid (BA) and ursolic acid (UA) (Figure 3.2) are naturally occurring triterpenoid which possess medicinal properties such as antifungal, antibacterial, antiviral, anti-HIV [34] and anti-tubercular activity [35].

In silico methods are a useful alternative approach in drug discovery and development. Besides speedy efficiency, this approach can be used to explain scenarios and answer questions that cannot be answered by physical chemistry methods. Molecular docking approach is applied to model ligand-receptor interaction, which permits characterization of their association and elucidation of fundamental biochemical processes involved [36]. Characterization of ligand-receptor association is essential in rational drug design [37]. MD simulations are useful as they show conformational evolution of a single molecule which is examined over time, whereas in the actual biological system, molecule conformational changes are demonstrated collectively [38].

Since compounds from *W. salutaris* exhibit antimycobacterial activity, there are possibilities it might inhibit mycobacterial QcrB. UA and UAA showed possible inhibition of mycobacterial QcrB. The binding of ligands to QcrB occurs mostly on the Q_P site and inhibition is more likely to occur in this site. However, there are many binding site in QcrB which are explored in this

46

study. We applied molecular modelling methods including molecular docking and MD simulations of *W. salutaris* compounds in complex with mycobacterial QcrB protein to answer questions in subject. We also conducted post-MD analyses of the simulated systems using specific methods, essentially MM/GBSA binding free energy calculations, to fulfil the aim of this study. Results of this study could pave way into directed experimental assessment of these compounds towards the development new TB drugs targeting QcrB protein, with minimum adverse effects, from cheap and freely accessible natural resources.
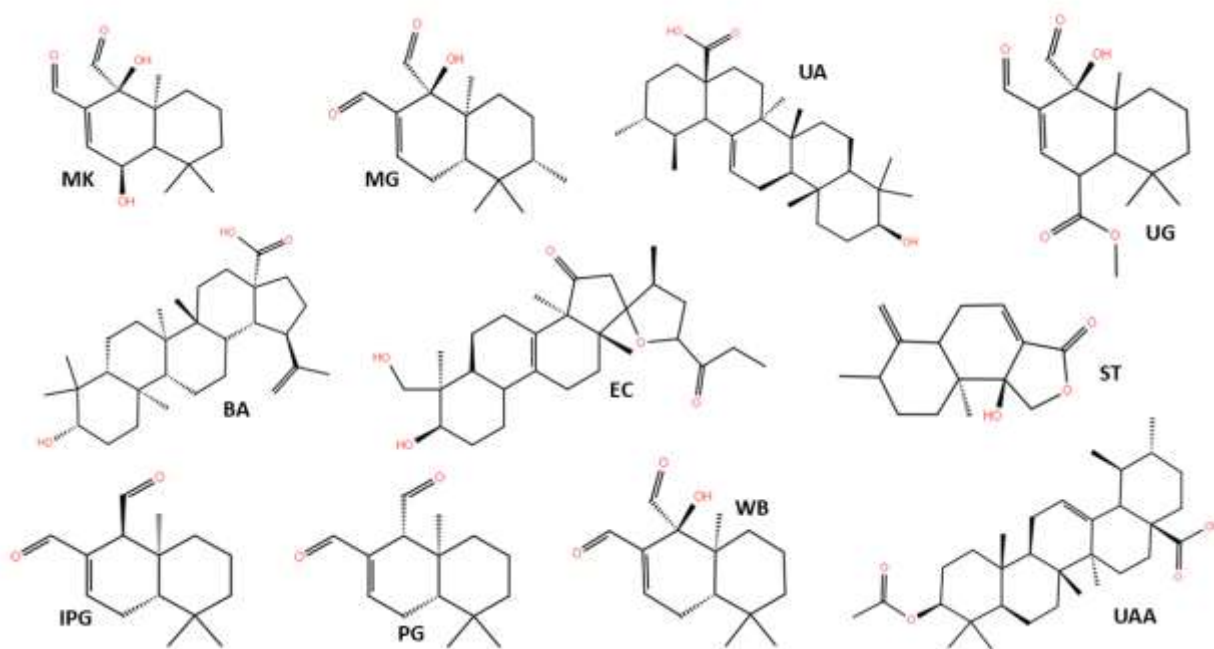
Figure 3.2: Structures of *W.salutaris* bioactive compounds modelled for inhibitory potential against *M.tuberculosis* QcrB.

.

3.2 Materials and Methods

3.2.1 Materials

A readily-modelled 3D crystal structure of *M. tuberculosis* QcrB (entry p9wp37) in complex with porphyrin ring structure was retrieved from UniprotKB (Swiss-prot) server [39]. Thirteen *W. salutaris* compound structures and Q203 drug were obtained from PubChem [40].

3.2.2 Molecular docking

The co-crystalized porphyrin structure was removed from QcrB prior to protein structure protonation at pH 7.4 in H++ web server [41]. Ligands were optimised using the steepest descent method and MMFF94s force field in Avogadro software [42]. UCSF Chimera [43] was used to add hydrogen atoms to the protein and to remove them from ligands. All ligands were docked into QcrB using AutoDock Vina [44]. Q203 and LSPZ were used as reference drugs. During docking, the partial charges of Gasteiger [45] were allotted. The AutoDock atom types were specified using the AutoDock graphical user interface given by MGL tools [46]. The grid box was defined by parameters of x = 126, Å y = 126 Å and z = 124 Å for the dimension while x = 199.86 Å, y = 175.72 Å and z = 213.139 Å for the centre grid and exhaustiveness = 8; with grid box spacing of 0.66 Å. The box encapsulated the whole protein structure to avoid biased ligand-binding. The Lamarckian genetic algorithm [47] was used to establish docked

conformations based on docking energies in a descending order. Docked complexes were then saved for MD simulations.

3.2.3   System settings for molecular dynamics simulations

Avogadro and UCSF Chimera software were respectively applied to add hydrogen atoms to ligands and to remove them from the receptor. MD simulations were performed using Sander Particle Mesh Ewald Molecular Dynamics (PMEMD) packaged in Amber14 [48]. A protein was described using an Amber force field ff12SB [49] [50]. To add hydrogen atoms to the protein as well as counter ions for the system neutralisation, the LEAP module in Amber14 was used [51]. The protein atoms are located 10 Å between the protein surface and the box boundary in each system found in the TIP3P water box [51]. In all the systems, boundary conditions of cubic periodicity were implemented. The non-bonding cut-off distance of 12 Å was used to treat long-range electrostatic interaction with particle mesh Ewald method [52] implemented in Amber14 . The whole system was minimised, applying a restraint potential of 500 kcal mol^{-1}Å^{-2}, for 1000 steps. The SANDER module of Amber14 software was used to perform unrestrained conjugated gradient minimization for 1000 steps for the entire system. With the aid of Langevin thermostat [53] at 1-ps random collision frequency, canonical ensemble (NVT) MD simulations were run for 50 ps while the system was progressively heated from 0 to 300 K with harmonic restraints of 5 kcal mol^{-1}Å^{-2} for solute atoms. The MD production simulation was performed at a constant temperature of 300 K and a constant pressure of 1 atm, using a time step of 2 fs and the Berendsen barostat [54] for constant pressure simulation. MD simulations of 200 ns were performed to get adequate sampling and systems convergence.

3.2.4   Post-dynamics analysis

49

Post-MD analysis was performed on generated trajectories using PTRAJ and CPPTRAJ module [55] implemented in Amber14 to evaluate root mean square deviation (RMSD), root mean square fluctuation (RMSF), radius of gyration (Rog) and ligand-residue interaction profile. The UCSF Chimera software was used to visualise the trajectories. Using Origin software [56], the findings were analysed and plots were generated.

3.2.5 Binding energy calculations

The binding free energy calculation is a method which provides valuable insight on binding affinity between the ligand and receptor [57]. It offers a detailed understanding of mechanism of binding, which includes both enthalpic and enthropic contributions to the molecular recognition [58]. Molecular Mechanics/Generalised-Born Surface Area (MM/GBSA) [57] was used to calculate the binding free energy of the ligands to QcrB. One thousand frames of a 200ns trajectory were used to calculate binding free energies. The following set of equations describes the binding free energy calculation:

$$\Delta G_{bind} = G_{complex} - G_{receptor} - G_{ligand} \tag{1}$$

$$\Delta G_{bind} = E_{gas} + G_{sol} - TS \tag{2}$$

$$E_{gas} = E_{int} + E_{vdW} + E_{ele} \tag{3}$$

$$G_{sol} = G_{GB} + G_{SA} \tag{4}$$

$$G_{SA} = \gamma SASA \tag{5}$$

From the above equations, E_{gas} represents the energy of the gas phase, E_{int} is the internal energy, E_{ele} represents Coulomb, while E_{vdW} is the van der Waals energies. E_{gas} is estimated directly from the ff12SB force field. G_{sol} which is the solvation free energy can be divided into two forms of contribution: polar and non-polar. The polar contribution is measured by solving the G_{GB} equation, while the non-polar solvation (G_{SA}) is calculated using solvent accessible surface area (SASA), which can be estimated from water probe radius of 1.4 Å. Standard mode analysis on specific conformational snapshot obtained from MD simulations is used to estimate the total entropy of the solute (S) and the temperature (T). The MM/GBSA binding free energy method in Amber14 evaluates the individual amino acid contribution to the total binding energy of the inhibitors and QcrB.

3.2.6   Principal component analysis

PCA defines the atomic displacement and conformational changes of the protein by extracting different modes of the conformation of the protein complex during dynamics simulations [59]. PTRAJ module in Amber 14 was used to strip solvent molecules and ions of the trajectories of all complexes from the 200ns trajectory. This was achieved prior to the PCA processing of MD trajectories. Using in-house scripts, PCA was applied on Cα atoms for 1000 snapshots at 100 ps time intervals. The first two principal components (PC1 and PC2) were computed and Cartesian coordinates of Cα atoms was used to generate 2×2 covariance matrices. PC1 and PC2 correspond to first two eigenvectors of covariance matrices. Origin software was used to construct PCA plots for QcrB-LSPZ, QcrB-Q203, QcrB-UA and QcrB-UAA systems.

3.2.7   Prediction of compound toxicity

Toxicity of UA and UAA was predicted using the pkCSM [60] online tool. Compound's SMILES obtained from PubChem were analysed using the pkCSM online tool. In addition, the

ProTox [61] online tool was used to predict its toxicity. This was performed to assess the LD50

value and classify compound's toxicity based on the Globally Harmonized System (GSH).

3.3   Results and Discussion

3.3.1   Molecular docking

Molecular docking aims at predicting the binding modes of the ligand by sampling its

orientation, conformation, and interactions when bound to an enzyme or another type of protein

receptor. Ligands were docked into the Mtb-QcrB structure (see table S1), where bind to the

protein at respective binding sites (Figure 3.3). The docking energies of the investigated

compounds ranged from -5.4 to -9.0 kcal/mol compared to LSPZ and Q203, which had energies

Figure 3.3: 3D structure of QcrB showing the binding position of LSPZ (green), Q203 (blue), UA (orange) and UAA

(cyan).

52

of -7.2 and -10.4 kcal/mol, respectively. UA and UAA showed a relatively higher docking energies of -8.9 and -9.0 kcal/mol, respectively. All ligands were further subjected to molecular dynamics analyses to determine the ligand–receptor models and accurate estimates of the binding affinities. Hence, docking alone cannot provide reliable results, it is of high importance to correlate docking results with MD simulations [62] [63][64].

MD simulations and analyses

UA, UAA, LSPZ and Q203 in complex with QcrB were subjected to MD simulations of 200 ns. Post-MD analyses namely root mean square deviation (RMSD), root mean square fluctuation (RMSF), radius of gyration (RoG), and binding free energy calculations were performed on trajectories of the simulated complexes and presented in the results section.

3.3.2   Systems stability

RMSD is an estimation that is widely used to describe the deviation of Cα atoms in protein residues, which is indicative of the degree of protein stability [65]. RMSD was calculated to assess the stability of simulated complexes, and the results are shown in Figure 3.4.
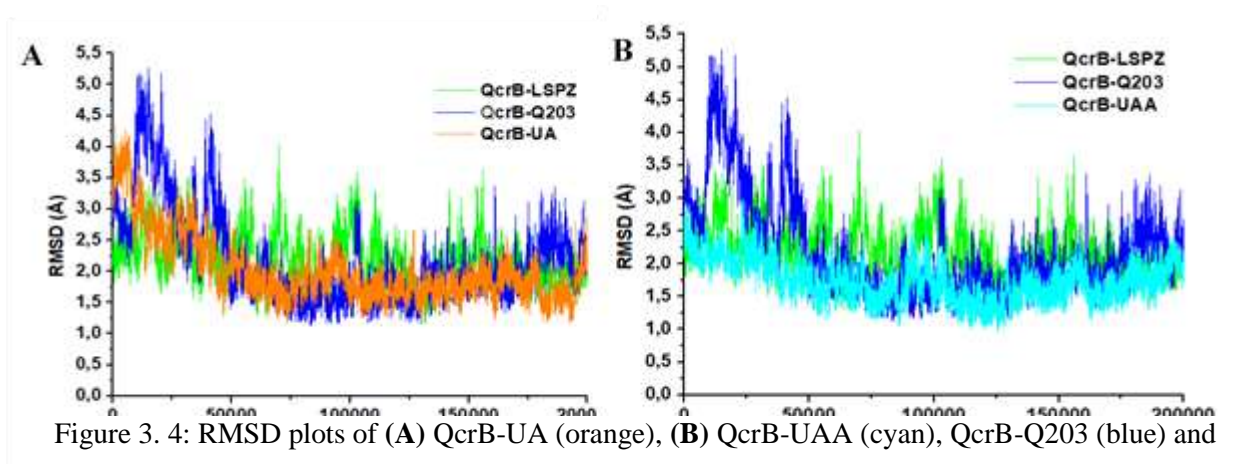
Figure 3. 4: RMSD plots of (**A**) QcrB-UA (orange), (**B**) QcrB-UAA (cyan), QcrB-Q203 (blue) and QcrB-LSPZ (green) complexes.

The average RMSD of QcrB in investigated complexes of UAA and UA was 1.7 Å to 1.9 Å compared to 2.1 Å for QcrB-LSPZ and QcrB-Q203 complexes (see table **S2**). QcrB-UA and QcrB-UAA complexes exhibited RMSD values less than 2. These complexes evidently proved to be more stable compared to reference drugs complexes, as a stable complex records an average RMSD value ≤ 2 Å. Many proteins are unstable in nature [66] [67] [68]. However, the binding of UA and UAA to QcrB contribute to complex stability.

3.3.3 Flexibility of ligand-receptor complexes

The mobility of amino acids in a protein gives insight to its dynamic behaviour during a MD simulation. This mobility is measured by calculating the root mean square fluctuation (RMSF), which measures the average mobility of amino acid atoms (N, Cα and C) during a MD simulation [69]. To explore the motion of the QcrB in association with the LSPZ, Q203, UA and UAA binding, RMSF was estimated, and results are plotted in Figure 3.5.
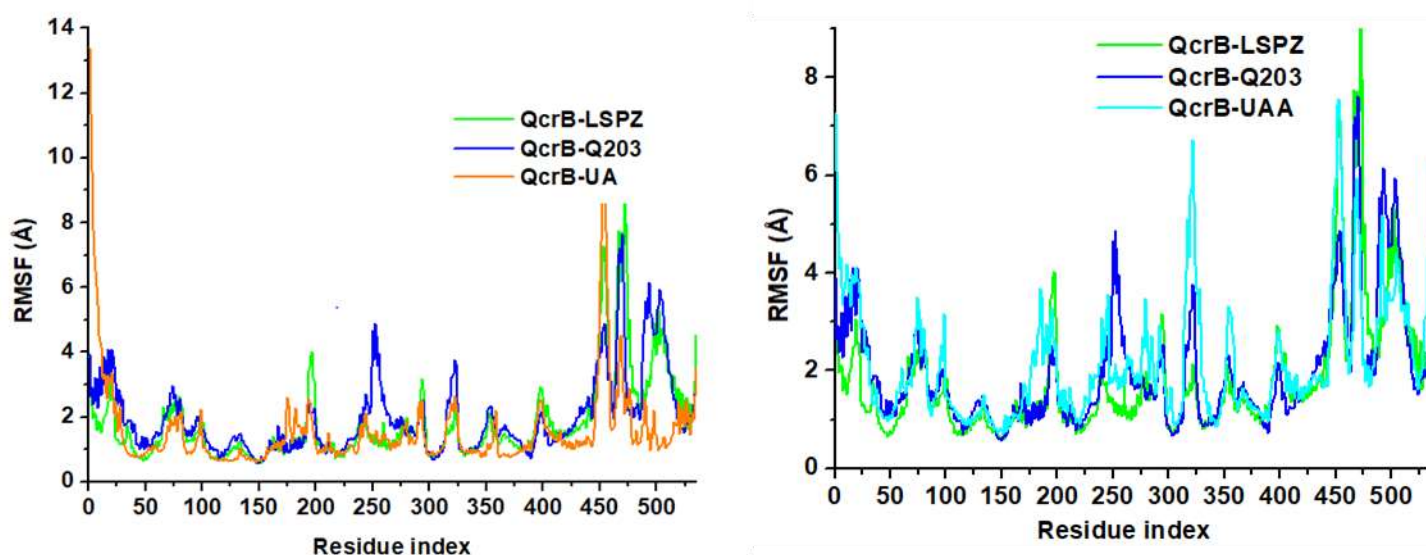
Figure 3. 5: The RMSF plots of **(A)** QcrB-UA (orange) and **(B)** QcrB-UAA (cyan) colours, respectively.

54

All conformations showed similar RMSF patterns throughout the 200ns simulation. Figure 3.5 and table S3 shows that the QcrB-UAA, QcrB-Q203 and QcrB-LSPZ has higher degree of flexibility compared to the QcrB-UA with an average RMSF of 2.1Å, 1.9Å, 1.8Å and 1.5Å, respectively. The most interesting observations are the amino acids that exhibit higher fluctuations, highlighted in Figure 3.5. Hence, these residues are located in the flexible loop of QcrB (Ile455-Ile464, Glu475-Gly477) [70]. In addition, Phe125, Phe127 [13], Thr128 [8] and Glu231 form part of the porphyrin ring binding site while Pro314 is located in the active site (Q_P) of QcrB [7]. As evident in Figure 3.5, it is clear that UA has altered the flexibility of most residues as compared to Q203, LSPZ and UAA. Generally, amino acids are flexible in nature and these findings are correlated to those reported, which suggested a large mobile loop of QcrB at position Ile455-Ile464, Glu475-Gly477 [70]. However, the presence of the UA in the active site was also found to impact the overall RMSF, as highlighted by lower average RMSF.

3.3.4   Radius of Gyration

Radius of gyration (RoG) is defined as the distribution of an object's components around the axis, it was used to provide an insight into the complex stability of the investigated systems. To measure the overall protein dimension of QcrB ligand-bound conformation, RoG was calculated, and results are presented in Figure 3.6 and table **S4**. The average RoG of QcrB in investigated complexes of UA and UAA was 27.5 Å to 27.8 Å as compared to QcrB-LSPZ and QcrB-Q203 complexes with 29.4 Å and 29.9 Å, respectively.
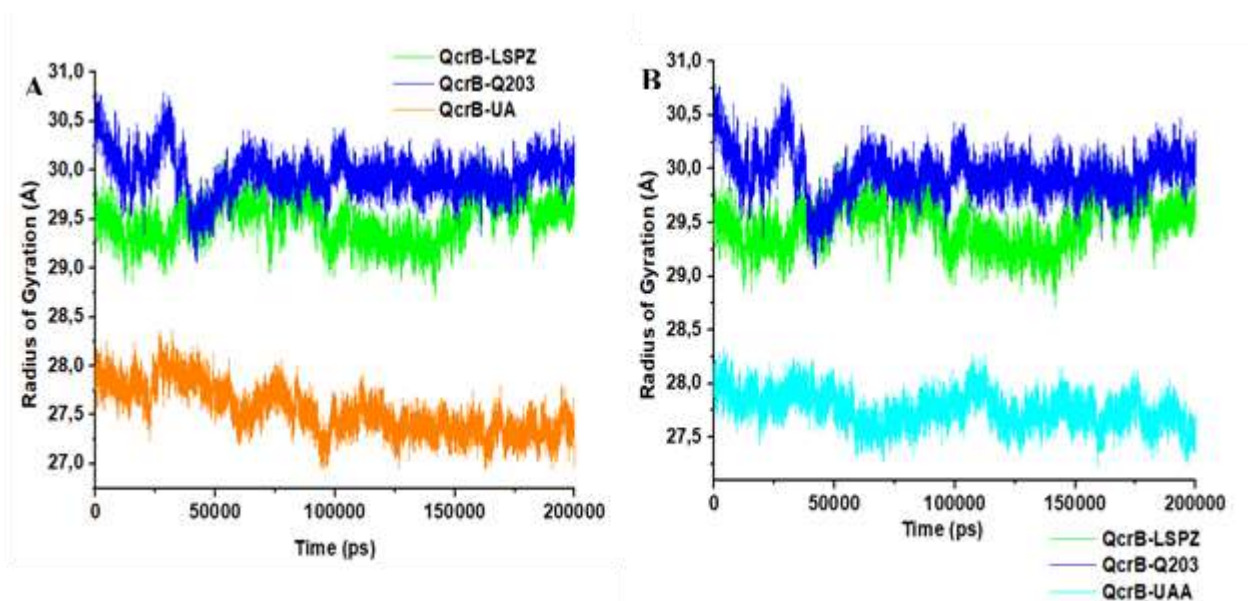
Figure 3.6: Radius of gyration plots **(A)** QcrB-UA (orange) and **(B)** QcrB-UAA (cyan) colours, respectively.

Results presented in figure 3.6 and table **S4** shows that QcrB exhibits more structural stability when it is bound to UA and UAA as compared to LSPZ and Q203. Hence, the attachment of UA and UAA inside QcrB porphyrin binding site leads to a conformational rigidity compared to LSPZ and Q203. These results are correlated to those of RMSF which justified a higher biomolecular flexibility of QcrB-UAA, QcrB-Q203 and QcrB-LSPZ structures as compared to QcrB-UA conformation. Hence, the QcrB structure is very flexible, and can be dynamically stabilized by UA.

3.3.5   Principal component analysis

PCA is a widely used method for investigating structural fluctuations in biological systems [59]. PCA was performed to understand the change of conformational diversities induced by the binding of various inhibitors. **Figure 3.7** shows differences in principal components of

QcrB-UA (A) and QcrB-UAA (B), versus control complexes QcrB-LSPZ and QcrB-Q203, defining distinctive QcrB structural conformations induced by bound ligands. QcrB-LSPZ and QcrB-Q203 complexes occupied a larger space and showed higher flactuation as compared to QcrB-UA and QcrB-UAA complexes. QcrB-UA and QcrB-UAA system exhibited a lesser fluctuation compared to reference drugs. These results indicate that QcrB-UA and QcrB-UAA complexes are more compacted compared to reference drugs complexes. These findings are consistent with those of RMSD and RoG, indicating that the binding of UA and UAA in QcrB results in complex stability and conformational rigidity compared to LSPZ and Q203.
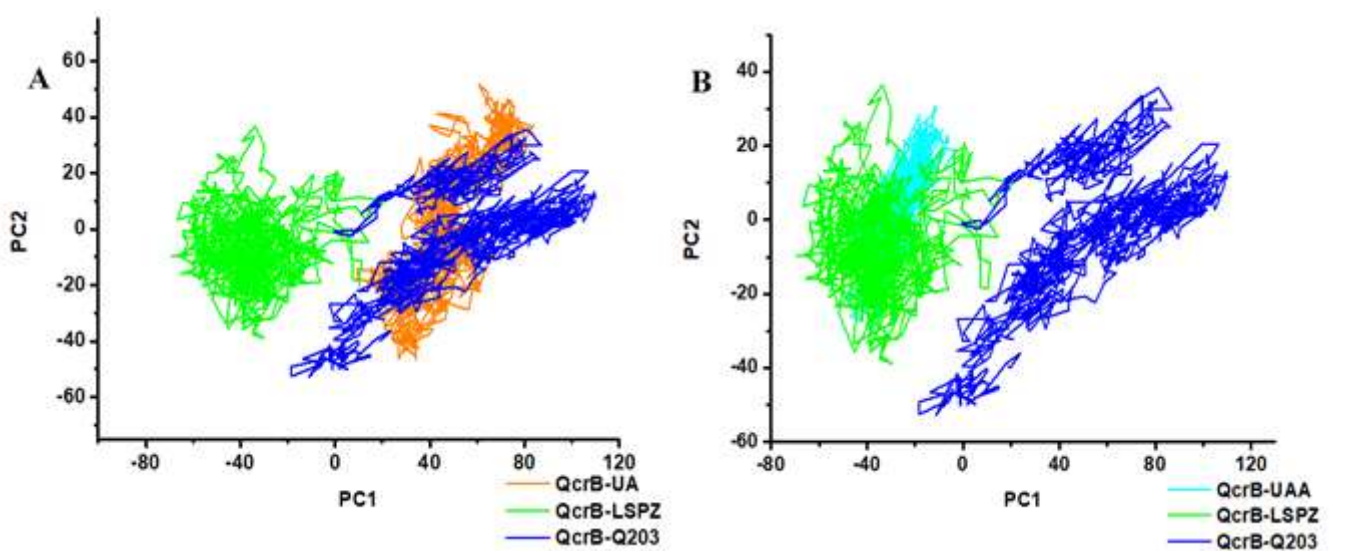
Figure 3.7: PCA projection of C-α atoms motion constructed by plotting the first two principal components (PC1 and PC2) in conformational space **(A)** QcrB-UA (orange) and **(B)** QcrB-UAA (cyan) colours, respectively.

3.3.6 Binding-free energy and energy decomposition analysis

MM/GBSA [57] method is a widely used approach to estimate the binding free energy of small ligands to biological macromolecules. MM/GBSA method was applied to calculate the binding free energy of UA, UAA, LSPZ and Q203 to QcrB, and the results are presented in **Table 1**. QcrB-UA had a highest total binding energy of -43.68 kcal/mol compared to QcrB-Q203 (-40.52 kcal/mol), QcrB-UAA (-28.42 kcal/mol) and QcrB-LSPZ (-26.45 kcal/mol). The binding free energy difference (-17.23 kcal/mol) between QcrB-UA and QcrB-LSPZ complex is quite significant.

The most interesting observation is that in QcrB-Q203 complex with an electrostatic energy and solvation energy of 28.76 kcal/mol and -22.46 kcal/mol, respectively. One feasible reason of this phenomenon is due to the presence of chlorine atoms in Q203 (see **Figure 3.1**). Hence, compounds with chlorine had been reported to display a negative solvation energy [71] [72]. Unfavourable solvation energy has also influenced the electrostatic energy.

In QcrB-UA complex, van der Waal's (-48.67 kcal/mol) forces, gas phase interaction (-51.29 kcal /mol) contributes significantly towards the total binding energy. Highest van der Waal's contribution may be due to the presence of numerous hydrophobic residue sidechains in QcrB binding site, which interact with multiple phenyl rings of UA resulting in hydrophobic packing. This defines a higher binding affinity of UA and consequently a stronger QcrB inhibition potential.

Table 1: MM/GBSA-based binding free energy profile of Q203, LSPZ, UA, and UAA on QcrB.

Complexes	ΔG_{bind} (Kcal/mol)	ΔE_{ele} (Kcal/mol)	ΔE_{vdW} (Kcal/mol)	ΔG_{gas} (Kcal/mol)	ΔG_{sov} (Kcal/mol)
QcrB-LSPZ	-26.45 ± 1.7	-1.65 ± 1.5	-34.15 ± 1.6	-35.81 ± 2.0	9.35 ± 1.4
QcrB-Q203	-40.52 ± 2.2	28.76 ± 5.1	-46.82 ± 1.9	-18.06 ± 5.9	-22.46 ± 5.2
QcrB-UA	-43.68 ± 4.0	-2.62 ± 1.8	-48.67 ± 3.9	-51.29 ± 4.0	7.61 ± 1.5
QcrB-UAA	-28.42 ± 2.4	-2.55 ± 1.6	-32.29 ± 2.3	-34.84 ± 3.0	6.42 ± 1.6

ΔE_{ele}, electrostatic energy; ΔE_{vdW}, van der Waals energy; ΔG_{gas}, gas phase interaction and ΔG_{sol}, solvation energy. The error bars were computed using MM/GBSA method.

3.3.7 Per-residue energy decomposition analysis

Amino acids involved in ligand-binding contribute to the calculated total binding energy. The contributions of van der Waals (ΔE_{vdw}) and electrostatic (ΔE_{ele}) interactions to the relative binding free energy of QcrB amino acids in association with the LSPZ, Q203, UA and UAA binding was estimated to obtain the total binding energy. Per-residue energy decomposition was performed for all simulated complexes and the results are presented in Figure 3.8-3.9 and table S5-S8.
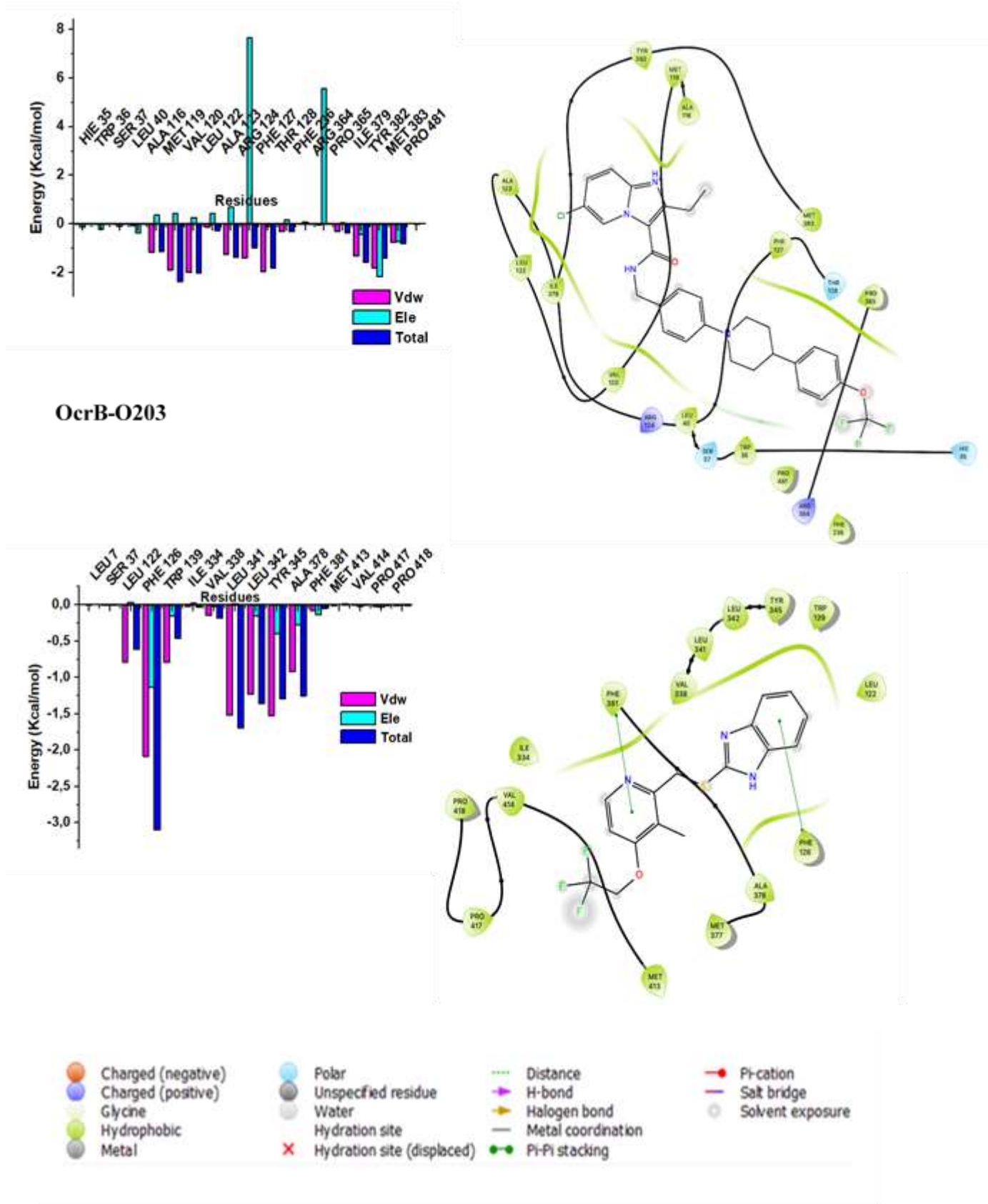
Figure 3. 8: The per-residue decomposition graphs and ligand-residue interaction map of QcrB-Q203 and QcrB-LSPZ complexes.
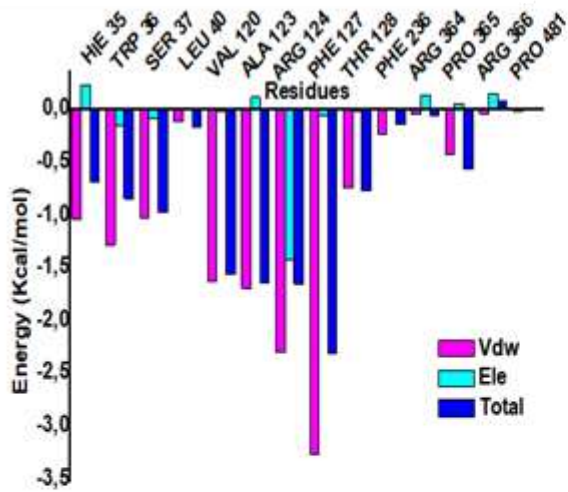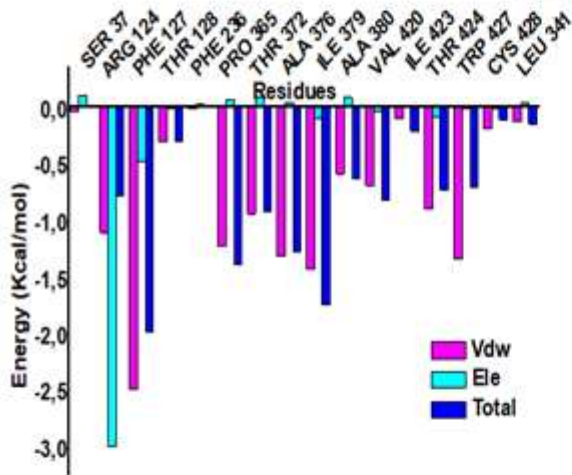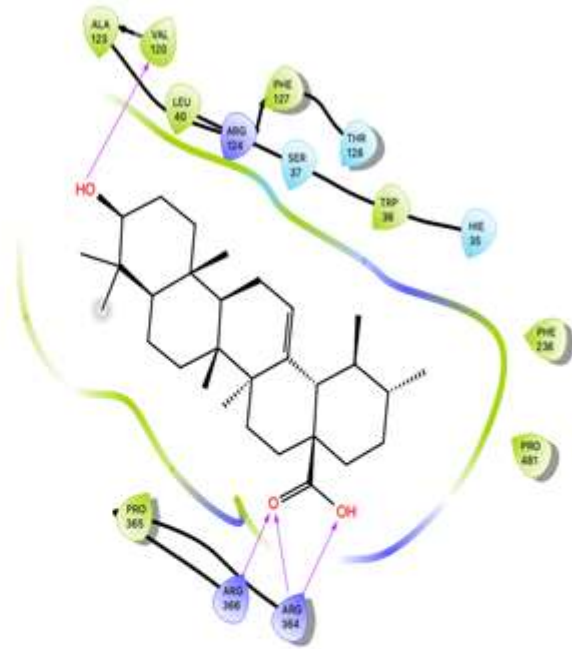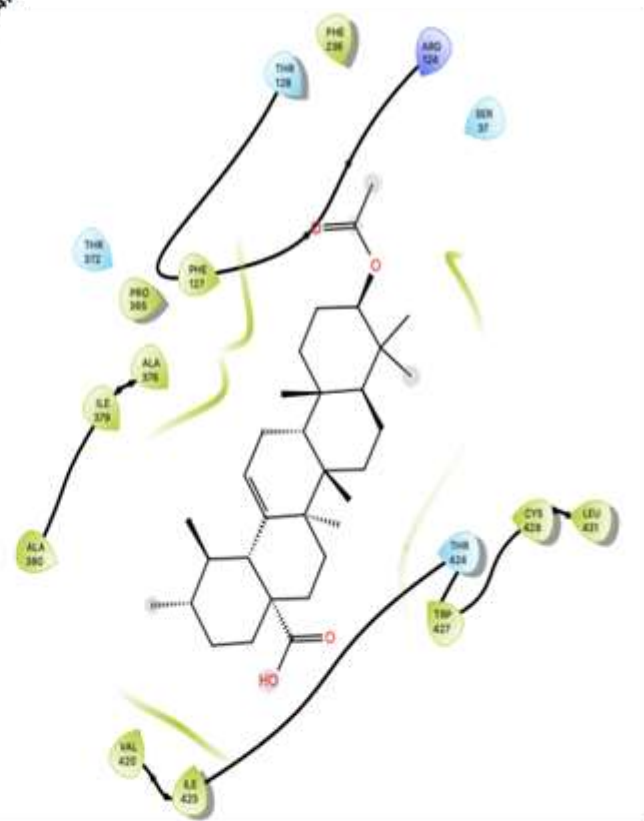
Figure 3.9: The per-residue decomposition graphs and ligand-residue interaction of QcrB-UA and

The larger total energy contributions (ΔG_{bind} > -2 kcal/mol) were from, Phe127, Met119, Phe126 in case of UA, Q203 and LSPZ, respectively. Phe127 in QcrB-UA complex contributed high van der Waals energy to overall binding free energy. This could be due to the interaction of hydrophobic residues with QcrB, which contains multiple UA phenyl rings. Hydrogen bonds were also observed in Val120, Arg364 and Arg366 for QcrB-UA complex.

Pharmacophore mapping approach is one of the reliable approaches in drug design. Interactions of candidate ligands with key residues of QcrB porphyrin binding site could assist in the development of a pharmacophore model for the identification and design of novel inhibitors targeting the porphyrin binding site in QcrB.

3.3.8 Predicted toxicity and biological activity

Drug toxicity is predicted on based on Ames test, inhibition of human hERG gene, hepatotoxicity and skin sensitivity [73]. The Ames test is a biological assay used to predict mutagenic potential of compounds using bacteria. The test is inexpensive, time-efficient, and plays a major role in new drug development for human use. The results of the estimated toxicity are shown in **Table 2.** Negative results obtained from Ames test for all compounds indicate a non-mutagenic sign. Inhibiting hERG can cause arrhythmia and more severe heart failure [74] [75][76] [77].

All compounds tested negative for hERG inhibition. One of the most dangerous aspects of drug development is drug-induced liver damage, which increases the rate of drug attrition [78]. Only UA displayed hepatotoxicity effect but no skin sensation was observed except in UAA. UA and UAA have high oral acute toxicity values (2.346 and 2.388 mol/kg, respectively). This

demonstrates high tolerance of compounds to recommended dose. Both the compounds exhibited reasonable toxicity properties.

Table 2: Predicted toxicity and biological activity of UA and UAA using pkCSM.

Compounds	UA	UAA
Ames toxicity	No	No
MTD	0.199	0.222
hERG I and II inh.	No	No
ORAT (LD50)	2.346	2.388
OCT	2.054	1.916
Hepatotoxicity	Yes	No
Skin sensation	No	No

MTD, maximum tolerated dose (human) (log mg/kg/day); hERG I and II inhibition, hERG inhibitor ORAT, oral rat acute toxicity (LD50) (mol/kg); OCT, oral chronic toxicity, chronic lowest-observed-adverse effect (LOAEL) (log/mg/kg_bw/day).

3.4 Conclusion

In this report, computational methods were applied to assess the probability of natural compounds isolated from *W.salutaris* as potential inhibitors of *M.tuberculosis* QcrB protein. These methods include Molecular Docking, MD simulation, radius of gyration (RoG), principal component analysis (PCA), Binding Free Energy calculations, Hydrogen bond formation and Toxicity Prediction were performed. The results of this study have revealed that UA has a higher binding affinity to QcrB compared to UAA, LSPZ and Q203. UA and UAA formed stable complexes with QcrB compared to LSPZ and Q203. UA had a highest binding energy compared to LSPZ and Q203, which resonated primarily from its interaction with

multiple hydrophobic amino acid residues in QcrB binding site. H-bonds formed between OH groups of UA and Val120, Arg364 and Arg366 of QcrB also contributed to UA binding affinity. Limited binding site residue mobility supported the binding affinity of UA to QcrB. UAA binds to porphyrin ring binding site with higher binding affinity compared to LSPZ. The observed binding affinity resonates primarily from van der Waals forces between UAA and hydrophobic residues of QcrB porphyrin ring binding site. This serves as an advantage since porphyrin ring contain heme which is involved in transportation of oxygen. UAA could potentially compete with porphyrin ring for the binding site and deprive the mycobacterial cell from oxygen, consequently disturbing mycobacterial oxygen-dependent metabolic processes. UA proved to be a superior compound; however, its estimated toxicity profile suggests that it is hepatotoxic within acceptable parameters. Therefore, finding a compound that compete with porphyrin ring for the same binding site may be useful in QcrB pharmocological studies. The preliminary report still warrants experimental validation to ascertain the presented findings

Authors' contributions:

Dr Ndumiso N. Mhlongo designed the research project, Ntombikayise Tembe participated in drafting and editing the manuscript, Kgothatso E. Machaba analysed the data, Hezekiel M. Kumalo and Umar Ndagi revised the manuscript. All authors read and approved the final manuscript.

Data availability

The dataset generated during the current study are available from the corresponding author on reasonable request.

Declarations

Conflict of interest: The authors declare no competing interests.

3.5 References

1. Popejoy, M. (2017). The Pandemic Nature of Reemerging Tuberculosis and the Role of Population Migration in its Spread. *MOJ Public Health*, *6*(4), 383–392. https://doi.org/10.15406/mojph.2017.06.00180

2. Macneil, A., Glaziou, P., Sismanidis, C., Maloney, S., & Floyd, K. (2019). Global epidemiology of tuberculosis and progress toward achieving global targets — 2017. *Morbidity and Mortality Weekly Report*, *68*(11), 263–266. https://doi.org/10.15585/mmwr.mm6811a3

3. World Health Organization. (2010). Multidrug and extensively drug-resistant TB (M/XDR-TB) 2010 Global Report on Surveillance and response. *Geneva, Switzerland.*

4. Berube, B. J., & Parish, T. (2018). Combinations of respiratory chain inhibitors have enhanced bactericidal activity against mycobacterium tuberculosis. *Antimicrobial Agents and Chemotherapy*, *62*(1), 1–10. https://doi.org/10.1128/AAC.01677-17

5. Matsoso, L. G., Kana, B. D., Crellin, P. K., Lea-smith, D. J., Pelosi, A., Powell, D., … Mizrahi, V. (2005). Function of the Cytochrome bc 1 - aa 3 Branch of the Respiratory Network in Mycobacteria and Network Adaptation Occurring in Response to Its Disruption. *Journal of Bacteriology*, *187*(18), 6300–6308. https://doi.org/10.1128/JB.187.18.6300

6. Lamprecht, D. A., Finin, P. M., Rahman, M. A., Cumming, B. M., Russell, S. L., Jonnala, S. R., … Steyn, A. J. C. (2016). Turning the respiratory flexibility of

Mycobacterium tuberculosis against itself. *Nature Communications*, *7*, 1–14. https://doi.org/10.1038/ncomms12393

7.   Ko, Y., & Choi, I. (2016). Putative 3D structure of *QcrB* from Mycobacterium tuberculosis cytochrome bc1 complex, a novel drug-target for new series of antituberculosis agent Q203. *Bulletin of the Korean Chemical Society*, *37*(5), 725–731. https://doi.org/10.1002/bkcs.10765

8.   Zhu, X. L., Zhang, R., Wu, Q. Y., Song, Y. J., Wang, Y. X., Yang, J. F., & Yang, G. F. (2019). Natural Product Neopeltolide as a Cytochrome bc 1 Complex Inhibitor: Mechanism of Action and Structural Modification. *Journal of Agricultural and Food Chemistry*, *67*(10), 2774–2781. https://doi.org/10.1021/acs.jafc.8b06195

9.   Pei-Liang Zhao , Le Wang, Xiao-Lei Zhu, Xiaoqin Huang, Chang-Guo Zhan, Jia-Wei Wu, G.-F. Y. (2010). Subnanomolar Inhibitor of Cytochrome bc1 Complex Designed via Optimizing Interaction with Conformationally Flexible Residues. *J Am Chem Soc*, *132(1)*, 185–194. https://doi.org/10.1021/ja905756c.

10.   Sassetti, C. M., Boyd, D. H., & Rubin, E. J. (2003). Genes required for mycobacterial growth defined by high density mutagenesis. *Molecular Microbiology*, *48*(1), 77–84. https://doi.org/10.1046/j.1365-2958.2003.03425.x

11.   Iqbal, I. K., Bajeli, S., Akela, A. K., & Kumar, A. (2018). Bioenergetics of mycobacterium: An emerging landscape for drug discovery. *Pathogens*, *7*(1). https://doi.org/10.3390/pathogens7010024

12.   Niebisch, A., & Bott, M. (2001). Molecular analysis of the cytochrome bc1-aa3 branch of the Corynebacterium glutamicum respiratory chain containing an unusual diheme cytochrome c1. *Archives of Microbiology*, *175*(4), 282–294. https://doi.org/10.1007/s002030100262

66

13. Hao, G., & Wang, F. et al. (2012). Computational Discovery of Picomolar Qo Site Inhibitors of Cytochrome bc1 Complex. *Journal of the American Chemical Society*, *134*, 11168−11176. https://doi.org/doi:10.1021/ja3001908

14. Schagger, H., Cramer, W. A., & Vonjagow, G. (1994). Analysis of Molecular Masses and Oligomeric states of Protein Complexes by Blue Native Electrophoresis and Isolation of Membrane Protein Complexes by Two-Dimensional Native Electrophoresis. *Analytical Biochemistry*, *217*(2), 220–230. https://doi.org/DOI: 10.1006/abio.1994.1112

15. Gao, X., & Wen, X. et al. (2002). The Crystal Structure of Mitochondrial Cytochrome bc1 in Complex with Famoxadone : The Role of Aromatic - Aromatic Interaction in Inhibition. *Biochemistry*, 11692–11702. https://doi.org/DOI: 10.1021/bi026252p

16. Crofts, A. R., Guergova-Kuras, M., Kuras, R., Ugulava, N., Li, J., & Hong, S. (2000). Proton-coupled electron transfer at the Q(o) site: What type of mechanism can account for the high activation barrier? *Biochimica et Biophysica Acta - Bioenergetics*, *1459*(2–3), 456–466. https://doi.org/10.1016/S0005-2728(00)00184-5

17. Abrahams, K. A., Cox, J. A. G., Spivey, V. L., Loman, N. J., Pallen, M. J., Constantinidou, C., … Besra, G. S. (2012). Identification of Novel Imidazo[1,2-a]pyridine Inhibitors Targeting M. tuberculosis *QcrB*. *PLoS ONE*, *7*(12). https://doi.org/10.1371/journal.pone.0052951

18. Rybniker, J., Vocat, A., Sala, C., Busso, P., Pojer, F., Benjak, A., & Cole, S. T. (2015). Lansoprazole is an antituberculous prodrug targeting cytochrome bc 1. *Nature Communications*, *6*(February 2017), 1–8. https://doi.org/10.1038/ncomms8659

19. Kalia, N. P., Hasenoehrl, E. J., Rahman, N. B. A., Koh, V. H., Ang, M. L. T., Sajorda, D. R., … Pethe, K. (2017). Exploiting the synthetic lethality between terminal

respiratory oxidases to kill Mycobacterium tuberculosis and clear host infection. *Proceedings of the National Academy of Sciences of the United States of America*, *114*(28), 7426–7431. https://doi.org/10.1073/pnas.1706139114

20.   Kinoshita, Y., Ishimura, N., & Ishihara, S. (2018). Advantages and disadvantages of long-term proton pump inhibitor use. *Journal of Neurogastroenterology and Motility*, *24*(2), 182–196. https://doi.org/10.5056/jnm18001

21.   Pandit, R., Singh, P. K., & Kumar, V. (2015). Natural Remedies against Multi-Drug Resistant <i>Mycobacterium tuberculosis</i> *Journal of Tuberculosis Research*, *03*(04), 171–183. https://doi.org/10.4236/jtr.2015.34024

22.   Nyaba, Z. N., Murambiwa, P., Opoku, A. R., Mukaratirwa, S., Shode, F. O., & Simelane, M. B. C. (2018). Isolation, characterization, and biological evaluation of a potent anti-malarial drimane sesquiterpene from Warburgia salutaris stem bark. *Malaria Journal*, *17*(1), 1–8. https://doi.org/10.1186/s12936-018-2439-6

23.   Van Wyk, B.E. van Oudshoorn, B. and Gericke, N. (2009). Medicinal plants of South Africa. *Journal of the South African Veterinary Association, 2nd edition.*, Pretoria, South Africa pp188. https://doi.org/doi: 10.4102/jsava.v81i3.145

24.   Madikane, V. E., Bhakta, S., Russell, A. J., Campbell, W. E., Claridge, T. D. W., Elisha, B. G., … Sim, E. (2007). Inhibition of mycobacterial arylamine N-acetyltransferase contributes to anti-mycobacterial activity of Warburgia salutaris. *Bioorganic and Medicinal Chemistry*, *15*(10), 3579–3586. https://doi.org/10.1016/j.bmc.2007.02.011

25.   Khamkar, A., Motghare, V., & Deshpande, R. (2015). Ethnopharmacology—a novel approach for drug discovery. *Indian J Pharm Pharmacol*, *2(4)*, 222–5. https://doi.org/DOI: 10.5958/2393-9087.2015.00007.2

26. Taniguchi, M., Yano, Y., Tada, E., Ikenishi, K., Oi, S., Haraguchi, H., Kubo, I. (1988). Mode of Action of Polygodial, an Antifungal Sesquiterpene Dialdehyde. *Agricultural and Biological Chemistry*, *52*(6), 1409–1414. https://doi.org/10.1080/00021369.1988.10868863

27. Mashimbye, M. J. (1993). Chemical constituents of plants native to Venda. Dissertation, University of Natal.

28. Frum, Y., & Viljoen, A. M. (2006). In vitro 5-lipoxygenase and anti-oxidant activities of South African medicinal plants commonly used topically for skin diseases. *Skin Pharmacology and Physiology*, *19*(6), 329–335. https://doi.org/10.1159/000095253

29. Frum, Y., Viljoen, A. M., & Drewes, S. E. (2005). In vitro 5-lipoxygenase and anti-oxidant activities of Warburgia salutaris and drimane sesquiterpenoids. *South African Journal of Botany*, *71*(3–4), 447–449. https://doi.org/10.1016/S0254-6299(15)30119-8

30. Mahmoud, I. ., Kinghorn, A. ., Cordell, A., & Farnsworth, N. (1980). Potential anticancer agents. XVI. Isolation of bicyclofarnesane sesquiterpenoids from Capsicodendron dinisii. *J Nat Prod.*, *43*(Suppl 3), 365–71.

31. Nakanishi, K., & Kubo, I. (1978). ChemInform Abstract: Studies on Warburganal, Muzigadial and Related Compounds. *Chemischer Informationsdienst*, *9*(14), 28–31. https://doi.org/10.1002/chin.197814354

32. Rabe, T., & Van Staden, J. (2000). Isolation of an antibacterial sesquiterpenoid from Warburgia salutaris. *Journal of Ethnopharmacology*, *73*(1–2), 171–174. https://doi.org/10.1016/S0378-8741(00)00293-2

33. Mashimbye, M. ., Maumela, M. ., & Drewes, S. (1999). A drimane sesquiterpinoid lactone from Warburgia salutaris. Phytochemistrye, *51*, 435–8.

34. Oloyede, H. O. B., Ajiboye, H. O., Salawu, M. O., & Ajiboye, T. O. (2017). Influence of oxidative stress on the antibacterial activity of betulin, betulinic acid and ursolic acid. *Microbial Pathogenesis*, *111*, 338–344. https://doi.org/10.1016/j.micpath.2017.08.012

35. Fadipe, V. O., Mongalo, N. I., Opoku, A. R., Dikhoba, P. M., & Makhafola, T. J. (2017). Isolation of anti-mycobacterial compounds from Curtisia dentata (Burm.f.) C.A.Sm (Curtisiaceae). *BMC Complementary and Alternative Medicine*, *17*(1), 1–6. https://doi.org/10.1186/s12906-017-1818-9

36. McConkey BJ, Sobolev V, E. M. (2002). The performance of current methods in ligand-protein docking. *Current Science.*, *83:845–855*.

37. Kitchen D.B., Decornez H., Furr J. R., & B. J. (2004). Docking and scoring in virtual screening for drug discovery: methods and applications. *Nat Rev Drug Discov*, *3*(11), 935–49. https://doi.org/doi: 10.1038/nrd1549.

38. F. S. Legge, A. Budi, H. T. and I. Y. (2006). Protein fexibility: multiple molecular dynamics simulations of insulin chain B, Biophys. *Chem*, *119*, 146–157.

39. Bairoch, A., & Apweiler, R. (1996). The SWISS-PROT protein sequence data bank and its new supplement TREMBL. *Nucleic Acids Research*, *24*(1), 21–25. https://doi.org/https://doi.org/10.1093/nar/24.1.21

40. Kim, S., Chen, J., Cheng, T., Gindulyte, A., He, J., He, S., Bolton, E. E. (2019). PubChem 2019 update: Improved access to chemical data. *Nucleic Acids Research*, *47*(D1), D1102–D1109. https://doi.org/10.1093/nar/gky1033

41. Gordon, J. C., Myers, J. B., Folta, T., Shoja, V., Heath, L. S., & Onufriev, A. (2005). H++: A server for estimating pKas and adding missing hydrogens to macromolecules. *Nucleic Acids Research*, *33*(SUPPL. 2), 368–371. https://doi.org/10.1093/nar/gki464

42.   Hanwell, M. D., Curtis, D. E., Lonie, D. C., Vandermeersch, T., Zurek, E., & Hutchison, G. R. (2012). Avogadro : an advanced semantic chemical editor , visualization , and analysis platform. *Journal of Chemoinformatics*, *4*(1), 17. https://doi.org/http://dx.doi.org/10.1186/1758-2946-4-17

43.   Pettersen, E. F., Goddard, T. D., Huang, C. C., Couch, G. S., Greenblatt, D. M., Meng, E. C., & Ferrin, T. E. (2004). UCSF Chimera — A Visualization System for Exploratory Research and Analysis. *J Comput Chem* ., *25*(13), 1605–12. https://doi.org/10.1002/jcc.20084

44.   Trott, O., & Olson, A. . (2010). AutoDock Vina: improving the speed and accuracy of docking with a new scoring function, efficient optimization and multithreading. *J Comput Chem.*, *31*(2), 455–461. https://doi.org/10.1002/jcc.21334

45.   Steffen, C., Thomas, K., Huniar, U., Hellweg, A., Rubner, O., & Schroer, A. (2010). TmoleX–a graphical user interface for TURBOMOLE. *Journal of Computational Chemistry*, *31*, 2967–2970.

46.   Huey, R., & Morris, G. M. (2005). Using AutoDock with AutoDockTools: a tutorial (1st ed.). *La Jolla: The script research institute molecular graphics laboratory.*

47.   Morris, G. M., Goodsell, D. S., Halliday, R. S., Huey, R., Hart, W. E., Belew, R. K., … Al, M. E. T. (1998). Automated Docking Using a Lamarckian Genetic Algorithm and an Empirical Binding Free Energy Function. *Journal of Computational Chemistry*, *19*(14), 1639–1662.

48.   Wang, J., Wolf, R. M., Caldwell, J. W., Kollman, P. A., & Case, D. A. (2004). Development and testing of a general amber force field. *J Comput Chem* ., *25*(9), 1157–74. https://doi.org/10.1002/jcc.20035

71

49.   Galindo-murillo, R., Robertson, J. C., Zgarbova, M., Jir, S., Otyepka, M., Jurec, P., & Cheatham, T. E. (2016). Assessing the Current State of Amber Force Field Modifications for DNA. *J. Chem. Theory Comput.*, *12*(8), 4114–4127. https://doi.org/10.1021/acs.jctc.6b00186

50.   Lindorff-larsen, K., Piana, S., Palmo, K., Maragakis, P., Klepeis, J. L., Dror, R. O., & Shaw, D. E. (2010). Improved side-chain torsion potentials for the Amber ff99SB protein force field. *Proteins*, *78*(8), 1950–1958. https://doi.org/10.1002/prot.22711

51.   Jorgensen, W. L., Chandrasekhar, J., Madura, J. D., Impey, R. W., Klein, M. L., Jorgensen, W. L., Klein, M. L. (1983). Comparison of simple potential functions for simulating liquid water. *J. Chem. Phys.*, *79*(2), 926–935. https://doi.org/10.1063/1.445869

52.   Harvey, M. J., & Fabritiis, G. De. (2009). An Implementation of the Smooth Particle Mesh Ewald Method on GPU Hardware. *J Chem Theory Comput .*, *5*(9), 2371–7. https://doi.org/10.1021/ct900275y

53.   Johnson, A., Johnson, T., & Khan, A. (2012). Thermostats in Molecular Dynamics Simulations An Interest in Thermostats. *University of Massachusetts Amherst, 1st edn*, 1–23.

54.   Finnerty, J. (2011). Molecular dynamics meets the physical world : Thermostats and barostats.

55.   Roe, D. R., & Cheatham, T. E. (2013). PTRAJ and CPPTRAJ: Software for Processing and Analysis of Molecular Dynamics Trajectory Data. *J. Chem. Theory Comput.*, *9*(7), 3084–3095. https://doi.org/10.1021/ct400341p

56.   Seifert, E. (2014). OriginPro 9.1: Scientific Data Analysis and Graphing Software -

Software Review. *Journal of Chemical Information and Modeling*, *54*, 1552–1552. https://doi.org/10.1021/ci500161d

57. Genheden, S., & Ryde, U. (2015). The MM / PBSA and MM / GBSA methods to estimate ligand-binding affinities. *Expert Opinion on Drug Discovery*, *10*(5), 10, 449– 461. https://doi.org/doi: 10.1517/17460441.2015.1032936

58. You, W., Huang, Y. M., Kizhake, S., & Natarajan, A. (2016). Characterization of Promiscuous Binding of Phosphor Ligands to Breast-Cancer-Gene 1 (BRCA1) C-Terminal (BRCT): Molecular Dynamics , Free Energy , Entropy and Inhibitor Design. *Computational Biology*, 1–25. https://doi.org/10.1371/journal.pcbi.1005057

59. David, C. C., & Jacobs, D. J. (2014). Principal component analysis: a method for determining the essential dynamics of proteins. *Methods in Molecular Biology, 1084*, 193–226. https://doi.org/https://doi.org/10.1007/978-1-62703- 658-0_11

60. Pires, D. E. V., Blundell, T. L., & Ascher, D. B. (2015). pkCSM: Predicting small-molecule pharmacokinetic and toxicity properties using graph-based signatures. *Journal of Medicinal Chemistry*, *58*(9), 4066–4072. https://doi.org/10.1021/acs.jmedchem.5b00104

61. Banerjee, P., Eckert, A. O., Schrey, A. K., & Preissner, R. (2018). ProTox-II : a webserver for the prediction of toxicity of chemicals, *46*(April), 257–263. https://doi.org/10.1093/nar/gky318

62. Cele, F. N., Ramesh, M., & Soliman, M. E. S. (2016). Per-residue energy decomposition pharmacophore model to enhance virtual screening in drug discovery: A study for identification of reverse transcriptase inhibitors as potential anti-HIV agents. *Drug Design, Development and Therapy*, *10*, 1365–1377. https://doi.org/10.2147/DDDT.S95533

73

63. Santos, L. H. S., Ferreira, R. S., & Caffarena, E. R. (2019). Integrating Molecular Docking and Molecular Dynamics Simulations. *Docking Screens for Drug Discovery, Methods in Molecular Biology, 2053*, 13–33. https://doi.org/https://doi.org/10.1007/978-1-4939-9752-7_2

64. Meng, X. Y., Zhang, H. X., Mezei, M., & Cui, M. (2011). Molecular docking: a powerful approach for structure-based drug discovery. *Current Computer Aided Drug Design*, *7*(2), 146–157. https://doi.org/10.2174/157340911795677602

65. Dixit, S. B., Ponomarev, S. Y., & Beveridge, D. L. (2006). Root Mean Square Deviation Probability Analysis of Molecular Dynamics Trajectories on DNA. *Journal of Chemical Information and Modeling*, *46(3)*, 1084–1093. https://doi.org/https://doi.org/10.1021/ci0504925

66. Molavi Tabrizi, A., Goossens, S., Mehdizadeh Rahimi, A., Knepley, M., & Bardhan, J. P. (2017). Predicting solvation free energies and thermodynamics in polar solvents and mixtures using a solvation-layer interface condition. *Journal of Chemical Physics*, *146*(9). https://doi.org/10.1063/1.4977037

67. Tompa, P. (2012). Intrinsically disordered proteins: a 10-year recap. *Trends Biochem. Sci.*, *37*, 509–516.

68. Deller, M. C., Kong, L., & Rupp, B. (2016). Protein stability: A crystallographer's perspective. *Acta Crystallographica Section:F Structural Biology Communications*, *72*, 72–95. https://doi.org/10.1107/S2053230X15024619

69. Vendome, J., Posy, S., Jin, X., Bahna, F., Shapiro, L., Honig, B., Avenue, N. (2011). HHS Public Access, *18*(6), 693–700. https://doi.org/10.1038/nsmb.2051.Molecular

70. Pan, Z., Wang, Y., Gu, X., Wang, J., & Cheng, M. (2019). Refined homology model of

cytochrome bcc complex B subunit for virtual screening of potential anti-tuberculosis agents. *Journal of Biomolecular Structure and Dynamics*, *1102*. https://doi.org/10.1080/07391102.2019.1688196

71.   Tomaník, L., Muchová, E., & Slavíček, P. (2020). Solvation energies of ions with ensemble cluster-continuum approach. *Physical Chemistry Chemical Physics*, *22*(39), 22357–22368. https://doi.org/10.1039/d0cp02768e

72.   McGrath, M. J., Kuo, I. F. W., Ngouana W., B. F., Ghogomu, J. N., Mundy, C. J., Marenich, A. V., Siepmann, J. I. (2013). Calculation of the Gibbs free energy of solvation and dissociation of HCl in water via Monte Carlo simulations and continuum solvation models. *Physical Chemistry Chemical Physics*, *15*(32), 13578–13585. https://doi.org/10.1039/c3cp51762d

73.   Han, Y., Zhang, J., Hu, C. Q., Zhang, X., Ma, B., & Zhang, P. (2019). In silico ADME and Toxicity Prediction of Ceftazidime and Its Impurities. *Front. Pharmacol*, *10*(434), 1–12. https://doi.org/10.3389/fphar.2019.00434

74.   Pearlstein, R. A., Vaz, R. J., Kang, J., Chen, X., Preobrazhenskaya, M., Shchekotikhin, A. E., Rampe, D. (2003). Characterization of HERG Potassium Channel Inhibition Using CoMSiA 3D QSAR and Homology Modeling Approaches. *Bioorg Med Chem Lett .*, *13*(10), 1829–1835. https://doi.org/10.1016/S0960-894X(03)00196-3

75.   Czodrowski, P. (2013). hERG Me Out. *J. Chem. Inf. Model.*, *53*(9), 2240–2251. https://doi.org/10.1021/ci400308z

76.   Sato, T., Yuki, H., Ogura, K., & Honma, T. (2018). Construction of an integrated database for hERG blocking small molecules. *PLoS ONE*, *13*(7), 1–18. https://doi.org/https://doi.org/10.1371/journal.pone.0199348

77.   Ferdinandy, P. (2019). Definition of hidden drug cardiotoxicity : paradigm change in cardiac safety testing and its clinical implications. *European Heart Journal*, *40*(22), 1771–1777. https://doi.org/10.1093/eurheartj/ehy365

78.   Ekowati, J., Diyah, N. W., Nofianti, K. A., & Hamid, I. S. (2018). Molecular Docking of Ferulic Acid Derivatives on P2Y 12 Receptor and their ADMET Prediction. *Journal of Mathematical and Fundamental Sciences*, *50*(2), 203–219. https://doi.org/10.5614/j.math.fund.sci.2018.50.2.8

4   CHAPTER 4

CONCLUSIONS AND FUTURE STUDIES

4.1   General conclusion

In this work, we conducted molecular docking and molecular dynamics simulations of UA, UAA, LSPZ, and Q203 ligands in a complex with *M. tuberculosis* QcrB protein to examine the inhibitory potential of UA isolated from *W. salutaris* and its derivative UAA. Our analysis has fully addressed the aim and objectives of this study. Based on their calculated binding affinities against QcrB, these compounds possess a greater inhibitory potential compared to the known drugs Q203 and LSPZ. They also possess appreciable adverse effects compared to the known drugs based on the predicted cytotoxicity profiles. This data could serve as the basis for further examination of the investigated compounds as preferred therapeutics targeting *M. tuberculosis* QcrB. This is also the first instalment reporting conformational and thermodynamic evolution of the investigated compounds using *in silico* methods.

4.2   Recommendation and Future Studies

Natural compounds are promising and lead to drug discovery, judging from the results obtained; the binding affinity of UA and UAA is higher compared to synthetic drugs. The porphyrin ring residues of QcrB contributed more to the total binding energy. This suggests that the ligands interacting with porphyrin binding site residues result in higher binding affinity compared to interactions in the active site. The removal of the porphyrin ring increased the affinity of ligands to interact with some of the residues located on its binding site. This is advantageous since the porphyrin ring contains heme, which is involved in oxygen transport.

This may result in the death of *M. tuberculosis* due to oxygen deprivation. Finding a compound/drug that competes with the porphyrin ring for the same binding site may thus be beneficial in QcrB pharmacological studies. However, the data generated from this study still warrant further experimental validation. As part of our future studies, we intend to express and purify mycobacterial QcrB for the examination and validation of the inhibitory properties expressed by the investigated compounds towards QcrB. This future study will provide cementing data to the conclusions made herein and more importantly present new compounds of natural descent as cheaply accessible therapeutics to treat TB.

Supplementary Information

Ursolic acid as a potential inhibitor of *Mycobacterium tuberculosis* cytochrome *bc1* oxidase ─ a molecular modelling perspective

Ntombikayise Tembe[1], Kgothatso E. Machaba[1], Umar Ndagi[2], Hezekiel M. Kumalo[1] and Ndumiso N. Mhlongo[1*]

[1]School of Laboratory Medicine and Medical Sciences, University of KwaZulu-Natal, Durban 4001, South Africa

[2]Africa Centre of Excellence for Mycotoxin and Food Safety, Federal University of Technology, Minna

* Corresponding author: Ndumiso N. Mhlongo

Email: mhlongon4@ukzn.ac.za

Telephone: +27(0) 31 260 2428, Fax: +27 031 260 7792

S 1: Docking energies of *W. salutaris* compounds complexed to *M. tuberculosis* QcrB.

Ligand	Docking Energy (kcal/ mol)
LSPZ	-7.2
Q203	-10.4
BA	-8.1
EC	-7.0
IPG	-5.9
MK	-5.4
MG	-5.8
PG	-5.4
ST	-6.2
UG	-5.8
UA	-8.9
UAA	-9.0
WB	-5.8

S 2: Average RMSD values of simulated complexes.

Complex	RMSD$_{avg}$ (Å)
QcrB-LSPZ	2.1 ± 0.7
QcrB-Q203	2.1 ± 0.4
QcrB-UA	1.9 ± 0.5
QcrB-UAA	1.7 ± 0.3

Data are expressed as mean $\pm$ SD, (n=200000)

S 3: Table of average RMSF values of simulated complexes.

Complex	RMSF$_{avg}$ (Å)
QcrB-LSPZ	1.8 ± 1.3
QcrB-Q203	1.9 ± 1.2
QcrB-UA	1.5 ± 1.4
QcrB-UAA	2.1 ± 1.2

Data are expressed as mean $\pm$ SD, (n=535)

S 4: Table of average RoG values of simulated complexes.

Complex	RoG$_{avg}$ (Å)
QcrB-LSPZ	29.4 ± 0.2
QcrB-Q203	29.9 ± 0.2
QcrB-UA	27.5 ± 0.2
QcrB-UAA	27.8 ± 0.2

Data are expressed as mean ± SD, (n=200000)

S 5: Table for per-residue energy decomposition of QcrB-LSPZ complex.

QcrB-LSPZ	ΔE_{vdw} (Kcal/mol)	ΔE_{ele} (Kcal/mol)	ΔG_{polar} (Kcal/mol)	$\Delta G_{non-polar}$ (Kcal/mol)	$\Delta G_{binding}$ (Kcal/mol)
Leu7	-0.000 ± 0.000	0.001 ± 0.001	-0.001 ± 0.001	0.000 ± 0.000	-0.000 ± 0.001
Ser37	-0.002 ± 0.001	0.004 ± 0.011	-0.004 ± 0.011	0.000 ± 0.000	-0.002 ± 0.006
Leu122	-0.786 ± 0.329	0.033 ± 0.187	0.180 ± 0.148	-0.038 ± 0.019	-0.611 ± 0.315
Phe126	-2.083 ± 0.331	-1.131 ± 0.450	0.280 ± 0.142	-0.167 ± 0.020	-3.100 ± 0.499
Trp139	-0.791 ± 0.322	-0.156 ± 0.134	0.559 ± 0.239	-0.076 ± 0.034	-0.464 ± 0.239
Ile334	-0.018 ± 0.003	0.023 ± 0.023	-0.035 ± 0.024	0.000 ± 0.000	-0.030 ± 0.009
Val338	-0.141 ± 0.037	-0.016 ± 0.044	-0.016 ± 0.053	-0.004 ± 0.015	-0.179 ± 0.061
Leu341	-1.521 ± 0.329	0.015 ± 0.131	0.126 ± 0.158	-0.317 ± 0.039	-1.697 ± 0.338
Leu342	-1.229 ± 0.287	-0.149 ± 0.089	0.265 ± 0.082	-0.248 ± 0.041	-1.361 ± 0.311
Tyr345	-1.526 ± 0.326	-0.396 ± 0.186	0.829 ± 0.186	-0.203 ± 0.026	-1.296 ± 0.312
Ala378	-0.922 ± 0.233	-0.271 ± 0.257	0.175 ± 0.159	-0.233 ± 0.038	-1.251 ± 0.360
Phe381	-0.074 ± 0.023	-0.138 ± 0.051	0.162 ± 0.049	-0.000 ± 0.002	-0.050 ± 0.023
Met413	-0.007 ± 0.002	-0.000 ± 0.024	0.020 ± 0.024	0.000 ± 0.000	0.013 ± 0.002
Val414	-0.004 ± 0.001	-0.022 ± 0.008	0.030 ± 0.009	0.000 ± 0.000	0.005 ± 0.002
Pro417	-0.021 ± 0.007	-0.031 ± 0.020	0.036 ± 0.019	0.000 ± 0.000	-0.015 ± 0.007
Pro418	-0.011 ± 0.003	0.001 ± 0.014	0.003 ± 0.015	0.000 ± 0.000	-0.008 ± 0.005

The binding energies were calculated using MMGBSA method.

S 6: Table of per-residue energy contribution of QcrB-Q203 complex.

QcrB-Q203	ΔE_{vdw} (Kcal/mol)	ΔE_{ele} (Kcal/mol)	ΔG_{polar} (Kcal/mol)	$\Delta G_{non-polar}$ (Kcal/mol)	$\Delta G_{binding}$ (Kcal/mol)
Hie35	-0.002 ± 0.001	-0.130 ± 0.052	0.133 ± 0.051	0.000 ± 0.000	0.001 ± 0.002
Trp36	-0.009 ± 0.005	-0.209 ± 0.028	0.224 ± 0.029	0.000 ± 0.000	0.006 ± 0.003
Ser37	-0.006 ± 0.003	-0.096 ± 0.045	0.112 ± 0.045	0.000 ± 0.000	0.010 ± 0.004
Leu40	-0.064 ± 0.023	-0.366 ± 0.043	0.418 ± 0.051	-0.001 ± 0.004	-0.013 ± 0.027
Ala116	-1.154 ± 0.228	0.368 ± 0.183	-0.072 ± 0.182	-0.265 ± 0.030	-1.122 ± 0.196
Met119	-1.904 ± 0.246	0.419 ± 0.329	-0.653 ± 0.471	-0.222 ± 0.041	-2.360 ± 0.433
Val120	-1.988 ± 0.243	0.252 ± 0.181	0.067 ± 0.183	-0.328 ± 0.027	-1.998 ± 0.290
Leu122	-0.124 ± 0.016	0.447 ± 0.058	-0.582 ± 0.088	0.000 ± 0.000	-0.259 ± 0.057
Ala123	-1.256 ± 0.240	0.681 ± 0.216	-0.666 ± 0.092	-0.117 ± 0.026	-1.359 ± 0.338
Arg124	-1.382 ± 0.371	7.645 ± 0.332	-7.042 ± 0.420	-0.198 ± 0.038	-0.977 ± 0.393
Phe127	-1.938 ± 0.365	-0.111 ± 0.191	0.470 ± 0.133	-0.219 ± 0.028	-1.797 ± 0.322
Thr128	-0.305 ± 0.093	0.150 ± 0.043	-0.116 ± 0.047	-0.040 ± 0.017	-0.312 ± 0.108
Phe236	-0.022 ± 0.008	0.078 ± 0.010	-0.068 ± 0.012	-0.000 ± 0.001	-0.012 ± 0.007
Arg364	-0.031 ± 0.010	5.554 ± 0.141	-5.508 ± 0.141	0.000 ± 0.000	0.015 ± 0.013
Pro365	-0.291 ± 0.129	0.038 ± 0.060	-0.006 ± 0.068	-0.106 ± 0.037	-0.365 ± 0.142
Ile379	-1.314 ± 0.256	-0.419 ± 0.107	0.465 ± 0.121	-0.294 ± 0.038	-1.562 ± 0.269
Tyr382	-1.802 ± 0.336	-2.174 ± 0.509	2.880 ± 0.455	-0.302 ± 0.054	-1.397 ± 0.322
Met383	-0.756 ± 0.334	-0.714 ± 0.666	0.851 ± 0.631	-0.173 ± 0.063	-0.791 ± 0.399
Pro481	-0.000 ± 0.000	-0.023 ± 0.018	0.023 ± 0.018	0.000 ± 0.000	-0.000 ± 0.001

S 7: Table of per-residue energy contribution of QcrB-UA complex.

QcrB-UA	ΔE_{vdW} (Kcal/mol)	ΔE_{ele} (Kcal/mol)	ΔG_{polar} (Kcal/mol)	$\Delta G_{non-polar}$ (Kcal/mol)	$\Delta G_{binding}$ (Kcal/mol)
Hie35	-1.034 ± 0.243	0.239 ± 0.469	0.232 ± 0.299	-0.114 ± 0.030	-0.678 ± 0.450
Trp36	-1.278 ± 0.294	-0.143 ± 0.128	0.735 ± 0.196	-0.157 ± 0.057	-0.842 ± 0.264
Ser37	-1.022 ± 0.164	-0.076 ± 0.095	0.181 ± 0.194	-0.056 ± 0.014	-0.973 ± 0.247
Leu40	-0.107 ± 0.020	0.016 ± 0.013	-0.073 ± 0.031	0.000 ± 0.000	-0.164 ± 0.036
Val120	-1.626 ± 0.321	-0.018 ± 0.057	0.219 ± 0.090	-0.134 ± 0.035	-1.558 ± 0.327
Ala123	-1.691 ± 0.349	0.118 ± 0.060	0.123 ± 0.112	-0.194 ± 0.033	-1.644 ± 0.354
Arg124	-2.301 ± 0.422	-1.414 ± 0.685	2.252 ± 0.891	-0.186 ± 0.035	-1.649 ± 0.657
Phe127	-3.265 ± 0.471	-0.056 ± 0.106	1.401 ± 0.273	-0.387 ± 0.032	-2.308 ± 0.375
Thr128	-0.735 ± 0.197	-0.011 ± 0.021	0.032 ± 0.059	-0.056 ± 0.020	-0.770 ± 0.213
Phe236	-0.232 ± 0.126	-0.005 ± 0.015	0.129 ± 0.050	-0.033 ± 0.028	-0.141 ± 0.113
Arg364	-0.043 ± 0.008	0.138 ± 0.089	-0.147 ± 0.092	0.000 ± 0.000	-0.051 ± 0.017
Pro365	-0.423 ± 0.222	0.056 ± 0.025	-0.036 ± 0.031	-0.158 ± 0.029	-0.562 ± 0.234
Arg366	-0.039 ± 0.014	0.155 ± 0.127	-0.036 ± 0.123	0.000 ± 0.000	0.080 ± 0.020
Pro481	-0.019 ± 0.006	-0.005 ± 0.007	0.025 ± 0.009	0.000 ± 0.000	0.001 ± 0.005

The binding energies were calculated using MMGBSA method.

S 8: Table of per-residue energy contribution of QcrB-UAA complex.

QcrB-UAA	ΔE_{vdW} (Kcal/mol)	ΔE_{ele} (Kcal/mol)	ΔG_{polar} (Kcal/mol)	$\Delta G_{non-polar}$ (Kcal/mol)	$\Delta G_{binding}$ (Kcal/mol)
Arg124	-1.111 ± 0.410	-3.006 ± 0.902	3.536 ± 0.868	-0.204 ± 0.069	-0.785 ± 0.303
Phe127	-2.493 ± 0.338	-0.476 ± 0.247	1.239 ± 0.218	-0.257 ± 0.028	-1.987 ± 0.307
Thr128	-0.307 ± 0.153	-0.013 ± 0.076	0.078 ± 0.079	-0.062 ± 0.022	-0.304 ± 0.163
Phe236	-0.011 ± 0.005	0.022 ± 0.008	-0.004 ± 0.007	0.000 ± 0.000	0.007 ± 0.003
Pro365	-1.228 ± 0.377	0.065 ± 0.064	0.028 ± 0.071	-0.249 ± 0.040	-1.385 ± 0.403
Thr372	-0.943 ± 0.208	0.088 ± 0.051	0.013 ± 0.115	-0.077 ± 0.015	-0.920 ± 0.200
Ala376	-1.319 ± 0.324	0.040 ± 0.059	0.137 ± 0.123	-0.136 ± 0.032	-1.279 ± 0.343
Ile379	-1.435 ± 0.336	-0.101 ± 0.141	0.014 ± 0.138	-0.229 ± 0.039	-1.752 ± 0.369
Ala380	-0.588 ± 0.228	0.088 ± 0.029	-0.071 ± 0.033	-0.057 ± 0.024	-0.628 ± 0.242
Val420	-0.690 ± 0.250	-0.033 ± 0.017	0.040 ± 0.049	-0.140 ± 0.032	-0.823 ± 0.269
Ile423	-0.102 ± 0.030	0.018 ± 0.017	-0.122 ± 0.045	-0.001 ± 0.004	-0.208 ± 0.060
Thr424	-0.903 ± 0.179	-0.083 ± 0.029	0.388 ± 0.124	-0.129 ± 0.027	-0.728 ± 0.175
Trp427	-1.341 ± 0.275	-0.013 ± 0.029	0.955 ± 0.174	-0.304 ± 0.035	-0.703 ± 0.220
Cys428	-0.187 ± 0.073	-0.008 ± 0.023	0.089 ± 0.062	-0.001 ± 0.002	-0.107 ± 0.054
Leu431	-0.131 ± 0.046	0.036 ± 0.011	-0.040 ± 0.019	-0.007 ± 0.012	-0.143 ± 0.056

ΔEele = electrostatic energy (kcal/mol); ΔEvdW = van der Waals energy (kcal/mol); ΔGpolar (kcal/mol) = polar solvation energy (kcal/mol), ΔGnon-polar (kcal/mol) = non-polar solvation energy (kcal/mol); ΔGbinding (kcal/mol) = total binding free energy (kcal/mol).

5 APPENDICES

A.1 Input files for docking in the *Mycobacterium tuberculosis* QcrB complexes.

receptor = rec.pdbqt

exhaustiveness = 8

center_x = 199.861

center_y = 175.722

center_z = 213.139

size_x = 126

size_y = 126

size_z = 124